

A novel *in silico* method to predict drug PK profile in human and its application to build the PBPK model of Hydroxychloroquine for COVID-19 treatment

by

Jingchen Zhai

Bachelor's degree, Changzhou University, 2019

Master's degree, University of Pittsburgh, 2021

Submitted to the Graduate Faculty of the
Click to choose your school in partial fulfillment
of the requirements for the degree of
Master of Science

University of Pittsburgh

2021

UNIVERSITY OF PITTSBURGH

SCHOOL OF PHARMACY

This thesis or dissertation was presented

by

Jingchen Zhai

It was defended on

March 26, 2021

and approved by

Dr. Junmei Wang, Associate Professor, Department of Pharmaceutical Sciences

Dr. Xiang-Qun Xie, Professor, Department of Pharmaceutical Science

Dr. Lirong Wang, Assistant Professor, Department of Pharmaceutical Sciences

Dr. Thomas D. Nolin, Associate Professor, Department of Pharmaceutical Sciences

Thesis Advisor: Junmei Wang, Department of Pharmaceutical Sciences

Copyright © by Jingchen Zhai

2021

A novel *in silico* method to predict drug PK profile in human and its application to build the PBPK model of Hydroxychloroquine for COVID-19 treatment

Jingchen Zhai, MS

University of Pittsburgh, 2021

The first part of this study is to develop a novel protocol to predict the pharmacokinetic profiles of a target drug based on the Physiologically based pharmacokinetic (PBPK) model of a structurally similar template drug by combining predictions from two software for PBPK modeling, the SimCYP simulator and ADMET Predictor. Thirteen drug pairs with Tanimoto similarity scores (TS) no less than 0.5 were studied. Three versions (V1, V2 and V3) of models using different predicted parameters for the target drug were constructed by replacing the corresponding parameters of the template drug step by step with those predicted by ADME Predictor for the target drug. Normalized Root Mean Square Error (NRMSE) was introduced for the evaluation of the model performance. Overall, for Group I drug pairs ($TS \leq 0.7$), V2 and V3 perform better than V1 in terms of NRMSE; for Group II drug pairs ($0.7 < TS \leq 0.9$), V3 outperforms the V1 and V2 versions. For the two drug pairs belong to Group III ($TS > 0.9$), V2 outperforms V1 and V3, suggesting more unnecessary replacement can lower the performance of PBPK models. We also investigated how the prediction accuracy of ADMET Predictor as well as its collaboration with SimCYP influence the quality of PBPK models constructed using SimCYP.

Hydroxychloroquine (HCQ) has been proposed as a promising treatment for COVID-19. To study the optimum dosing regimens for HCQ on COVID-19 that can balance its therapeutic efficacy and cardiac side-effect, we constructed a PBPK model for HCQ based on the method we proposed above and deducted the therapeutic window for COVID-19. To enable drug plasma

concentration to reach the treatment level at the beginning of the treatment, we proposed to administrate HCQ either 600 mg BID or 800 mg BID first. Also, the maintaining dose of 400 mg BID or 200 mg TID in the following treatment is found necessary to maintain the drug plasma level until the 7th day. Drug concentrations in the heart and lung were also deducted to reflect dosing efficacy and to avoid the potential risk of cardiotoxicity. Reduced dosing regimens have also been proposed for the elderly and the renal impairment population.

Table of Contents

Preface.....	xiii
1.0 Introduction.....	1
1.1 Current situation under COVID-19 pandemic.....	1
1.2 PBPK modeling techniques in drug development	2
1.3 A novel method proposed for predicting drug PK profile.....	3
1.4 PBPK modeling for Hydroxychloroquine	4
2.0 Methods.....	6
2.1 The proposed method to predict drug PK profile	6
2.1.1 Drug preparation	6
2.1.2 Structure similarity calculation	6
2.1.3 Validation of PBPK models for drug templates	7
2.1.4 Evaluation of Inherent differences among software platforms	8
2.1.5 Model construction for target drugs	8
2.1.6 Evaluation of models for target drugs.....	9
2.2 PBPK modeling for HCQ and optimized dosing regimens for COVID-19.....	10
2.2.1 The PBPK model construction and verification for HCQ	10
2.2.2 2 Dose regimens for different population and extrapolated drug organ concentration	11
3.0 Results	13
3.1 The proposed method to predict drug PK profile	13
3.1.1 Drug pairs selection and validation of PBPK models for drug templates	13

3.1.2 Evaluation of Inherent differences among software platforms	16
3.1.3 Predicted concentration profiles for the in silico PBPK models.....	21
3.2 PBPK Modeling for HCQ and optimized dosing regimens as a potential treatment for COVID-19	26
3.2.1 The PBPK model for HCQ.....	26
3.2.2 Simulation on different dosage regimens ranging from COVID treatment effective dose to cardiotoxicity dose.....	27
3.2.3 Predicted PK profile for proposed dosing regimens	29
3.2.4 Application of promising dosing regimens to special populations.....	33
3.2.4.1 Recommendation A: Regimen 4 (600 mg BID for two days, followed by 400 mg BID)	33
3.2.4.2 Recommendation B: Regimen 8 (600 mg BID for three days, followed by 400 mg BID)	35
3.2.4.3 Recommendation C: Regimen 14 (800 mg BID for two days, followed by 200 mg TID)	36
3.2.4.4 Recommendation D: Regimen 12 (800 mg BID for two days, followed by 400 mg BID)	37
3.2.4.5 Recommendation E: Regimen 15 (800 mg BID for two days + 400 mg BID for one days + 200 mg TID)	39
3.2.4.6 Recommendation F: Regimen 16 (800 mg BID for two days + 400 mg BID for two days + 200 mg TID)	40
3.2.4.7 Adjusted dosing regimens for renal impairment populations.....	41
3.2.4.8 Adjusted dosing regimens for the elder population.....	43

4.0 Discussion.....	45
4.1 A New Approach for In Silico Prediction of Oral Drug Concentration Profiles in Human for Drug Candidates Lack Experimental Pharmacokinetic Data.....	45
4.1.1 The practical guidance on selecting suitable drug template	45
4.1.2 Another possible method to evaluate the prediction results of the three versions.....	46
4.1.3 The perspective of applying <i>in silico</i> PBPK modeling for compounds lack experimental ADME and PK properties.....	47
4.2 Simulation on different dosage regimens ranging from COVID treatment effective dose to cardiotoxicity dose	48
5.0 Conclusions.....	53
5.1 An approach to predict oral drug concentration profiles for drug candidates lack experimental PK data.....	53
5.2 PBPK modeling HCQ and proposed dosing regimens for healthy population and special populations as a potential treatment for COVID-19	54
Appendix A Supplementary.....	56
Appendix A.1 Supplementary Tables	56
Appendix A.2 Supplementary Figures	69
Bibliography	72

List of Tables

Table 1	Current software platforms for PK modeling	4
Table 2	Input parameters for HCQ PBPK model	11
Table 3	The calculated Tanimoto Coefficient between each pair of drugs	13
Table 4	The comparison between predicted and observed PK profiles of all drugs	17
Table 5	Calculated NRMSE between predicted results by modified drug template and experimental concentration profiles of drugs.....	21
Table 6	Calculated NRMSE between predicted (three versions) and experimental concentration profiles of drugs in each group.....	24
Table 7	A series of dosing regimens proposed in this study.....	29
Table 8	Regimens for the elder population and two renal impairment populations.....	43
Table S1	Input parameters for 18 drugs (predicted by ADMET Predictor)	56
Table S2	Modified parameters predicted by ADMET Predictor for Fluoxetine template... 	59
Table S3	Predicted PK parameters by SimCYP Simulator of each group.....	60
Table S4	The predicted maximum drug concentration and the corresponding time during two dosing periods of dosing regimen 4.....	61
Table S5	The predicted maximum drug concentration and the corresponding time during two dosing periods of dosing regimen 8	62
Table S6	The predicted maximum drug concentration and the corresponding time during two dosing periods of dosing regimen 14	63

Table S7 The predicted maximum drug concentration and the corresponding time during two dosing periods of dosing regimen 12	64
Table S8 The predicted maximum drug concentration and the corresponding time during three dosing periods of dosing regimen 15	65
Table S9 The predicted maximum drug concentration and the corresponding time during three dosing periods of dosing regimen 16	66
Table S10 The predicted maximum drug concentration and the corresponding time during three dosing periods of adjusted dosing regimen for the two renal impairment population	67
Table S11 The predicted maximum drug concentration and the corresponding time during three dosing periods of adjusted dosing regimen for the elder population	68

List of Figures

**Figure 1 The predicted concentration profiles by SimCYP and observed data of all drugs.
..... 15**

**Figure 2 The predicted concentration profiles using SimCYP drug template with input
parameters from ADMET Predictor and observed data of all drugs..... 20**

**Figure 3 The predicted concentration profiles of three versions and observed data of all
predicted drugs..... 25**

Figure 4 Validation of HCQ model within 3 days (left) and 7 days (right). 26

**Figure 5 Drug plasma concentration under different dosage regimens, with each regimen
colored with a different color 27**

**Figure 6 The predicted drug plasma C-T curved for a series of dosing regimens reported in
clinical trials. 28**

**Figure 7 The time course of plasma drug concentration for Regimens 1-8 which administer
600 mg BID for first 1-3 days..... 30**

**Figure 8 The time course of drug plasma concentration for Regimens 9-16 which administer
800 mg BID for first 1-3 days..... 32**

**Figure 9 Predicted drug concentration profiles for different populations in plasma, heart,
and lung under recommended dosing Regimen 4..... 34**

**Figure 10 Predicted drug concentration profiles for different populations in plasma, heart,
and lung under recommended dosing Regimen 8..... 36**

**Figure 11 Predicted drug concentration profiles for different populations in plasma, heart,
and lung under recommended dosing Regimen 14..... 37**

Figure 12 Predicted drug concentration profiles for different populations in plasma, heart, and lung under recommended dosing Regimen 12..... 38

Figure 13 Predicted drug concentration profiles for different populations in plasma, heart, and lung under recommended dosing Regimen 15..... 40

Figure 14 Predicted drug concentration profiles for different populations in plasma, heart, and lung under recommended dosing Regimen 16..... 41

Figure 15 Predicted drug concentration profiles for two renal impairment populations in plasma, heart, and lung under two adjusted dosing regimens 43

Figure 16 Predicted drug concentration profiles for the elder population in plasma, heart, and lung under two adjusted dosing regimens..... 44

Figure S1 Predicted drug concentration profiles for the renal impairment population (GRF) in plasma under Regimens 1, 2, 3, 5, 6, 7, 9, 10, 11 and 13..... 69

Figure S2 Predicted drug concentration profiles for the renal impairment population (GRFL) in plasma under Regimens 1, 2, 3, 5, 6, 7, 9, 10, 11 and 13..... 70

Figure S3 Predicted drug concentration profiles for the elder population (NEC) in plasma under Regimens 1, 2, 3, 5, 6, 7, 9, 10, 11 and 13..... 71

Preface

Before going to college, I used to have an idea in mind that things could be digitized and described by mathematical models. During my undergraduate education, when learning about computer-aided drug design for the first time, I found that the idea of using computational methods to design and improve drugs coincided with my original belief. When I learned that I had the opportunity to join this Master program, I decided to have my Master research related to this direction without hesitation. I was too much excited about my decision because I loved to face the challenge and have a try at something I never engaged in but always believed in. My experience at Pitt proved that I would never regret making that choice.

Within nearly two years, I have the chance to know a series of advanced knowledge and skills relying on the high efficiency and power of the computer during the research. I am equipped with PBPK modeling skills and molecular modeling skills. It has been shown to me how powerful computational tools can be and how to utilize them during several projects I have engaged in, but I know that this is only the tip of the iceberg. I feel so lucky that I can receive training from both the research field, and it is my great fortune to continue researching both of them during my PhD training in Pitt with my current advisor, Dr. Wang. Although these two fields seem separate, the power of combining them can be imagined. A door has been open to me, and it's my pleasure to have the ticket into the knowledge palace.

I would like to thank my advisor Dr. Junmei Wang very much for giving me very generous support during my research. I would like to thank Dr. Sean Xie for giving me the chance to join our wonderful Master program as well as providing so many research resources. I would like to also thank Dr. Lirong Wang for his support and concern during my Master training. Thank Dr.

Thomas Nolin for providing valuable suggestions during a PBPK project. And thank these four professors so much for being my committee members and their suggestions to this thesis. Thanks a lot to other professors in our School of Pharmacy for their help, and thank my families and friends for their support during my two-year study and life.

1.0 Introduction

1.1 Current situation under COVID-19 pandemic

The coronavirus disease 2019 (COVID-19) caused by the novel severe acute respiratory syndrome coronavirus 2 (SARS-CoV-2),[1,2] has caused over 17,592,760 cases within the US since January 21, 2020. The disease has claimed death to the 315,260 people[3], and is still ongoing because of its high infectivity. Noteworthy, individuals with many common diseases, such as cardiac diseases, hypertension, diabetes, and other people who are being treated with ACE2-increasing drugs, are more susceptible to the SARS-CoV-2[4]. Also, co-morbid tends to worsen the patients' prognosis.[5,6] Thus, a feasible treatment is urgently needed to deal with this severe condition. Currently, the only drug with FDA's approval for emergency use aiming at COVID-19, remdesivir,[7] has been reported a lot of side-effects and possesses much debate on its efficacy.[8,9] Although a large volume of clinical trials was launched to find potential therapeutic regimens,[10] there is still no other therapy for this infectious disease proven to be effective in clinical currently.

Drug repurposing is a very promising method for searching for potential drugs as treatments of a newly emerged disease in a short time. Besides remdesivir, a great diversity of already proved drugs have been tested for the therapeutic efficacy evaluation in COVID-19 clinical treatment, including hydroxychloroquine, chloroquine, ritonavir, lopinavir, and many other drugs[11-14]. However, clinical tests and observations for drug efficacy still request much time and a large number of patients involved in. Furthermore, without knowing the proper dosing

regimens, the drug treatment maybe less efficient and a potential risk due to drug toxicity may increase.

1.2 PBPK modeling techniques in drug development

Pharmacokinetics is the study of the time courses of a drug administered to the body, which includes the processes of absorption, distribution, metabolism and excretion (ADME).[15] Usually, it is essential to quantitatively measure the concentration of the drug in plasma at different time points in pharmacokinetic (PK) study, for the analysis of drug behavior and dose adjustment. In addition to clinical trials which always involved time cost and ethical considerations, the “measurement” of concentration profiles under various administration conditions can also be achieved by the implementation of Physiologically based pharmacokinetic (PBPK)[16-18] modeling with known PK parameters related to drug properties or its ADME profiles. On the other hand, computational tools for both PBPK modeling and PK parameter prediction have been developed, further reducing experimental cost. Therefore, by virtue of such tools, the quick and convenient *in silico* prediction of drug behavior in human body can be easily performed without investing much effort in experiments, informing further studies in drug toxicity, dosing strategy and potential drug-drug interactions. As such, this *in silico* method can be particularly useful in preclinical study and can serve as a tool to help select drug candidates which are more likely to have desirable PK profiles.

1.3 A novel method proposed for predicting drug PK profile

In this study, we developed a novel method to predict the concentration profile of a target compound based on PBPK models constructed using the model of a structurally similar drug which serves as the template. Among current software platforms (**Table 1**), we utilized the SimCYP Simulator (V19, Release 1; Shefeld, UK)[19] software to construct PBPK models for a target drug by only substituting the predicted ADME parameters of the target drug for those applied by the PBPK model of the corresponding template drug. We applied ADMET Predictor (V9.5, Simulation Plus),[20,21] a software developed by SimulationPlus Inc. to predict the ADME properties of target drugs, which include physiochemical parameters like fraction unbound in plasma (F_u) and blood-to-plasma partition ratio (B/P), and ADME input parameters such as the volume of distribution (V_d), Michaelis-Menten constant (K_m) and maximal metabolism rate (V_{max}) of common enzymes. Meanwhile, to better validate our constructed PBPK models as well as evaluate the performance of the two software tools, we selected 18 drugs collected by SimCYP compound library (including substrates and inhibitors) as the template drugs. In total, 13 drug pairs were formed based on their structural similarity. For each pair of drugs, one serves as the template and the other as the target drug. For the target drug in a drug pair, we pretended that no PBPK model was available for it and new PBPK models were constructed based on the PBPK model of the template drug. We tested three protocols by introducing ADME Predictor predicted ADME properties into the template PBPK model and evaluated the model performance using the observed PK profile of the target drug. The corresponding PBPK models constructed using the three protocols, in brief, were called V1, V2 and V3 models, respectively.

Table 1 Current software platforms for PK modeling

Software	Availability
SimCYP Simulator	Commercially available
Phoenix WinNonlin	Commercially available
GastroPlus	Commercially available
NONMEN	Commercially available
PK sim	Open source
Matlab	Commercially available
ADMET Predictor	Commercially available
PKanalix	Academic free
Simulx	Academic free
Monolix	Academic free

1.4 PBPK modeling for Hydroxychloroquine

Since hydroxychloroquine (HCQ) has been nominated by Donald Trump, this drug has aroused much attention among the public and underwent a series of in vitro and in vivo tests as a potential treatment of COVID-19, with its efficacy reports varying. Chloroquine also received much concern because of its highly similar properties to hydroxychloroquine. However, compared to chloroquine, hydroxychloroquine has less cardiotoxicity, more solubility, and a higher tolerable dose[22-27]. The FDA proved therapeutic dosages of HCQ ranges from 200 mg a day to 800 mg as the first dose following by a lower dosage, dosing regimens varying in different diseases as treatments, such as Malaria and Rheumatoid arthritis (not include COVID-19), and the mechanism of action is still unknown.[28] Although some research claimed that hydroxychloroquine tends to show no significant treatment effect along with severe side effects,[29,30] growing evidence indicates that the viral load can significantly be inhibited by HCQ with a higher dose such as 600 mg BID, with the main side effect, QT interval prolongation, occurring only at an extremely high

dose. [27,31-35] Thus, it is imperative to study the maximum safe dose of hydroxychloroquine to avoid the cardiotoxicity of this drug.

From previous studies, researchers have attempted to build a PBPK model for HCQ based on mice experiments and clinical data.[36] The relationship between drug plasma concentration and lung concentration has also been researched based on monkey experiment data.[37] However, as a treatment for COVID-19, the administration of HCQ still lacks clinical dosing guidance and the relationship between dosing, plasma concentration, and cardiotoxicity is still unknown. What's more, for different special populations taking this drug, such as the elderly population and pregnant population, how to adjust their dosing regimens is also unknown.

In this study, we used *in silico* method to build the PBPK model of hydroxychloroquine and predict the PK profiles of HCQ with a series of dosing regimens. Drug concentration profiles in different organs were also predicted based on this PBPK model to speculate drug peak concentrations in specific organs, including heart and lung. The drug peak concentration in heart should serve as a risk indicator of cardiotoxicity while that in lung can help to predict drug treatment efficacy at the COVID-19 targeted organ. According to the currently reported HCQ cardiotoxic dose, we deduced a series of dosing regimens that balanced treatment effect and the risk of its most severe side effect - prolonged QT interval. Moreover, as a potential treatment for pneumonia disease, drug concentration at lung under respective dosage scenarios was also predicted. What's more, for SARS-CoV-2's strong infectious ability and wide susceptible populations, we compared the predicted PK profiles between cohorts with different physiology or pathology models to come up with adjusted dosing regimens for different populations.

2.0 Methods

2.1 The proposed method to predict drug PK profile

2.1.1 Drug preparation

Drugs selected for the construction of in silico PBPK models come from the built-in drug database of the SimCYP software. Simplified Molecular-Input Line-Entry System (SMILES)[38] strings of all drugs from SimCYP built-in library, including substrates and inhibitors, were collected from the DrugBank database (<https://www.drugbank.ca/>). The SMILES strings of drugs were used not only for their structural similarity calculation on a web platform, but also as inputs for the generation of their properties using ADMET Predictor.

2.1.2 Structure similarity calculation

Tanimoto scoring is a commonly used method to compute the fingerprint-based similarity between two compounds.[39] In this study, we applied the maximum common substructure-based (MCS) Tanimoto algorithm for the similarity calculation. The Tanimoto score (TS) is defined by the function below:[40]

$$TS(X, Y) = \frac{N_Z}{N_X + N_Y - N_Z}$$

Where N_X and N_Y are the numbers of bits in fragment bit-strings of the two compounds, and N_Z is the intersection set, i.e., the number of common substructures shared by these two compounds. $TS(X, Y)$ ranges from 0 to 1, measuring the structural similarity between two

compounds from the lowest to the highest (when the two molecules are identical). TS scores were calculated using ChemMine (<https://chemminetools.ucr.edu/similarity>) for all combinations of drugs in the SimCYP compound database.

2.1.3 Validation of PBPK models for drug templates

We first validated the PBPK models of all selected 18 drugs by utilizing their observed data from literature. In detail, we utilized the original built-in models of those drugs in SimCYP to run the simulation. In terms of the trial design, the dose regimens, simulation time as well as population information including age, weight and health condition were the same as those reported in the clinical study of PK measurement. Meanwhile, the parameters of the built-in PBPK model, like the drug's ADME properties, remained the same for all the drugs except for Fluoxetine. As a racemate, we adjusted some of its ADME and PK parameters according to the literature to make the predicted curve much better fitting the experimental data.[41-43] The key ADME parameters predicted by ADME Predictor for the 18 drugs were all listed in **Table S1**, and the detailed input information for Fluoxetine template is shown in **Table S2**. The observed drug concentration data of each template drug was extracted from published concentration-time (C-T) curves using WebPlotDigitizer (<https://automeris.io/WebPlotDigitizer/>). The C-T curves from simulations were then overlaid to the observed drug concentrations. The predicted PK profiles of each template drug, including the maximal concentration (C_{Max}), the time at which C_{Max} is observed (T_{Max}), and area under the curve (AUC), were compared to the observed ones.

2.1.4 Evaluation of Inherent differences among software platforms

The quality of models constructed for target drugs not only affected by the structural similarity between the template drug and the target drug, but also relies on the prediction quality of ADMET Predictor and how well the collaboration is between the two software. There may be some inherent differences among different software platforms, including but not limited to the training set data and algorithms for constructing models. More importantly, the prediction accuracy of ADMET Predictor for an individual ADME parameter is unknown. Thus, we utilized parameters predicted by ADMET Predictor for the 18 drugs to simulate their PK profiles using SimCYP and then compared them to those predicted using SimCYP built-in parameters. The following ADME parameters predicted by ADMET Predictor were evaluated: molecular weight (MW), B/P, f_u , the logarithm of the octanol-buffer partition coefficient ($\log P_{o:w}$), acid dissociation constant (pK_a), human jejunum effective permeability (P_{eff}), V_d , and Cytochrome P450 (CYP) metabolism parameters (K_m , V_{max} or CL_{int}). The values of these ADME parameters for 18 drugs are listed in **Table S1**.

2.1.5 Model construction for target drugs

In total, three versions of PBPK models for a target drug were built by modifying the models of the template drug: (1) in Version 1 (V1), only the MW of template drug was changed to that of the target one; (2) in Version 2 (V2), in addition to the MW, the physiochemical properties, including B/P, f_u , $\log P_{o:w}$ and pK_a of the template drug were replaced by the ones predicted of the target drug; (3) in Version 3 (V3), in addition to MW and physiochemical properties, the input parameters for ADME process, including P_{eff} in absorption, V_d in distribution,

Cytochrome P450 (CYP) metabolism parameters (K_m , V_{max} or CL_{int}) of templates were all replaced with the calculated ones for the target drug. All the ADME properties of the target drugs are predicted by ADMET Predictor, a software tool that can predict over 140 properties based on its built-in Quantitative structure-activity relationship (QSPR) models.[44] Information about the experimental subjects and the trial design of each target drug during simulations was derived from the corresponding clinical reports.

2.1.6 Evaluation of models for target drugs

To evaluate the performance of PBPK models with input parameters from ADMET Predictor, the experimental data of each drug were overlaid by the simulated C-T curves of this drug. To quantitatively evaluate how well the experimental and simulated curves are overlaid with each other, we calculated the root mean square error (RMSE)[45] of the observed and predicted concentrations at different time points. The formula for the RMSE calculation is as follow:

$$RMSE = [\sum_{i=1}^N (C_{pi} - C_{oi})^2 / N]^{1/2}$$

Where C_{oi} and C_{pi} represent the observed and predicted drug concentration at the time point i . N is the number of time points ($N > 1$) from the extracted observed data. Specifically, in this study, to facilitate the comparison between models for different drugs with various concentration scales, we introduced normalized RMSE (NRMSE) to evaluate the performance of PBPK models, which is calculated using the following formula:

$$NRMSE = \frac{RMSE}{C_{max} - C_{min}}$$

Where C_{max} and C_{min} are the maximum and minimum values among the observed and predicted concentrations using all three versions of models.

2.2 PBPK modeling for HCQ and optimized dosing regimens for COVID-19

2.2.1 The PBPK model construction and verification for HCQ

In this study, a PBPK model for HCQ was developed using SimCYP Simulator. Because parameters of some enzyme activity are unavailable in clinical and preclinical reports, we used ADMET Predictor 9.5 to predict metabolizing enzyme activity. Meanwhile, the advanced compartmental and transit (ACAT) model, which is utilized in the ADMET Predictor software to predict drug exposure,[46] shares the most similarity with the advanced dissolution, absorption, and metabolism (ADAM) model adopted to analyze drug absorption in SimCYP. Thus, we chose the ADAM model to analyze drug distribution during the simulation. A full PBPK model was used to analyze drug distribution in the heart and lung. Bellow mentioned “drug organ concentration” all refer to heart and lung drug concentration.

Before building the PBPK model for HCQ, we first calculated the Tanimoto score between HCQ and drugs (including substrates and inhibitors) in the SimCYP drug library. Among the limited drugs in the SimCYP database with well-built templates, Ciprofloxacin shares the highest Tanimoto score with HCQ, 0.3056, thus was selected as a template to construct the HCQ PBPK model. Except for available property descriptions of drugs collected from literature reports and predicted metabolizing parameters, absent or unclear information of HCQ, including B/P, F_u , and the p-gp (ABCB1) transporter were adjusted and compromised with each other within the range reported in the literature to fit the clinical reported PK curve of HCQ. [47-56] Details of input parameters have been shown in **Table 2**.

Table 2 Input parameters for HCQ PBPK model

<i>Parameter</i>	<i>Input Value</i>
Physiochemical Properties	
Molecular weight (g/mol)	335.872 ^a
LogP	3.6 ^b
pKa	9.67 ^b
Blood Binding	
B/P	0.55 ^e
F _u	0.1 ^e
Absorption (ADAM model)	
P _{eff} (10 ⁻⁴ cm/s)	2.32 ^c
PSA (Å ²)	48.39 ^a
Distribution (Full PBPK model)	
V _{ss} (L/kg)	18.12 (Method 1) ^c
Elimination	
CYP1A2	V _{max} : 7.928, K _m : 20.777 ^d
CYP2D6	V _{max} : 2.319, k _m : 14.602 ^d
Transporter	
p-gp (ABCB1)	Cl _{int} : 18 ^e

B/P: blood-to-plasma partition ratio. F_u: the fraction of unbound drug in plasma. P_{eff}: human jejunum effective permeability. PSA: polar surface area. V_{ss}: volume of distribution at steady state using tissue volumes for a population representative of healthy volunteer population. V_{max}: maximum rate of metabolism (pmol/min/pmol of isoform). K_m: Michaelis-Menten constant, (μM). a: data from DrugBank. b: data from Pubmed. c: SimCYP Prediction result. d: ADMET Predictor prediction result. e: fit clinical curve

2.2.2 2 Dose regimens for different population and extrapolated drug organ concentration

With the constructed HCQ model, we conducted a series of simulations to study drug plasma levels under different dosage regimens. Combining with the results of HCQ treatment aiming at COVID-19 from many clinical trials, we thus extrapolated the safe and effective drug plasma concentration level from clinical recommended dosing regimens for the normal population. Corresponding organ concentrations of the drug were also predicted under recommended dosages

to prevent cardiotoxicity caused by HCQ. Based on simulation results of recommended dosing regimens for the virtual healthy population in SimCYP Simulator software, simulations were conducted under different virtual populations in SimCYP library and the concentration-time (C-T) curves for different populations were also predicted. Special populations include GRF (renal impairment population, $30 \text{ mL/min} \leq \text{GRF} \leq 60 \text{ mL/min}$), GRFL (renal impairment population, $\text{GRF} \leq 30 \text{ mL/min}$), MO (morbidly obese population), NEC (geriatric Northern European Caucasians population), Obe (obese population), Preg (pregnant population), RA (rheumatoid arthritis population) and Norm (healthy volunteers). For renal impairment populations, (morbidly or not) obese population, elderly population, and pregnant population, these are most common special populations which have different physical conditions from healthy subjects and thus may need special adjustment for dosing regimens. The reason the RA population was taken into special consideration is that HCQ is a drug proved to treat RA patients, and these patients should have a special ADME response to HCQ.[57] To analyze how each dosing regimens affect patient plasma and organ drug concentration, the predicted maximum drug concentration during each dosing stage, and the corresponding time was compared and analyzed.

3.0 Results

3.1 The proposed method to predict drug PK profile

3.1.1 Drug pairs selection and validation of PBPK models for drug templates

13 pairs out of 18 drugs, which have the calculated TS equal to or better than 0.5, were selected for the *in silico* PBPK modeling. Drug pairs with TS below 0.5 were not considered to be structurally similar and were excluded in this study. The calculated TS for selected 13 pairs (Groups A-M) were listed in **Table 3**. Since both drugs in a pair will in turn serve as the template and target drug for cross-validation, we used X-1 and X-2 to label two drug pair sets, respectively, where X can be A to M.

Table 3 The calculated Tanimoto Coefficient between each pair of drugs

Group	Drug 1	Drug 2	Tanimoto score
A	Bupropion	Dextromethorphan	0.50
B	Bufuralol	Bupropion	0.52
C	Dextromethorphan	Quinidine	0.57
D	Lorazepam	Midazolam	0.63
E	Alprazolam	Lorazepam	0.65
F	Lorazepam	Triazolam	0.69
G	Mephenytoin	Phenobarbital	0.74
H	Atomoxetine	Fluoxetine	0.78
I	Simvastatin	Pravastatin	0.82
J	Triazolam	Midazolam	0.84
K	Midazolam	Alprazolam	0.88
L	Theophylline	Caffeine	0.93
M	Imipramine	Desipramine	0.95

The predicted mean plasma concentration-time profiles overlaid with observed data of all 18 template drugs are shown in **Figure 1**. Accordingly, **Table 4**[43,58-73] exhibits the predicted

PK parameters (C_{Max} , T_{Max} , AUC) versus observed values. From **Table 4**, excluding the drugs with observed PK parameters all unavailable (Dextromethorphan, Mephenytoin and Fluoxetine), the predicted PK parameters of most drugs are within the standard deviation ranges of their observed values. The predicted mean values of C_{Max} , T_{Max} and AUC for Theophylline are all slightly beyond the margin of error but still within the range of two-fold standard deviation. Overall, as shown in **Figure 1**, the observed C-T profiles are within the 95% Confidence Interval (CI) ranges (the upper and lower grey dashed curves) of the simulated C-T curves. Therefore, the PBPK models for the template drugs have been well validated.

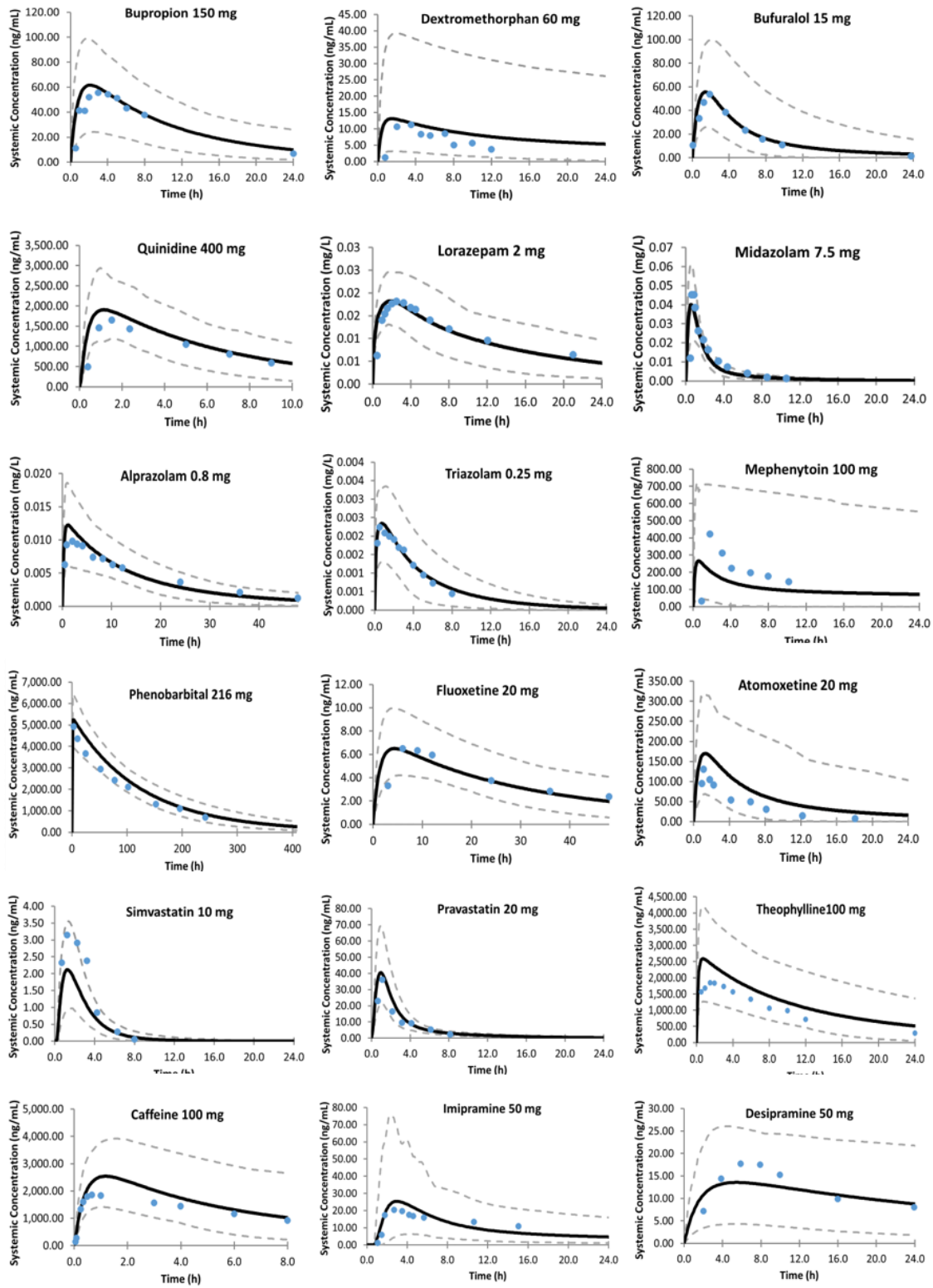


Figure 1 The predicted concentration profiles by SimCYP and observed data of all drugs.

Prediction results for all drugs except Fluoxetine are from the original SimCYP template. The result for Fluoxetine is from adjusted Fluoxetine template. Upper and lower dashed grey curves represent 95 % confidential interval.

3.1.2 Evaluation of Inherent differences among software platforms

The predicted PK parameters of the 18 modified drug templates by replacing the ADME parameters with those predicted by ADMET Predictor are listed in **Table 4**. The C-T profiles of those 18 drugs are shown in **Figure 2**. It is demonstrated that Bupropion, Caffeine, and Phenobarbital show a very good overlay between the clinical reports and predicted results from modified drug templates, with the observed data laying within the confidence interval of the predicted curve. As to Fluoxetine, Alprazolam, Quinidine, and Triazolam, although the predicted results do not show an excellent overlay with the experimental data, most of the clinical data points lays within the confidence interval of the prediction profiles. For Lorazepam, although the observed data all at or around the upper confidence interval of the predicted profile, the shape of the predicted curve shares a high similarity with that of the observed PK profile. Unfortunately, the other drugs do not show very satisfying prediction results, using clinical data points as references.

To quantitatively measure the deviation of predicted concentration profiles from the experimental data, the difference between observed and predicted values are evaluated by NRMSE (**Table 4**). The lower the NRMSE value is, the smaller the difference between the predicted and experimental concentration profile is, i.e., the better performance the created model for the drug is. The top three drugs, Caffeine, Phenobarbital, and Bupropion, all have very small NRMSE values, which is consistent with the fact that the simulated C-T curves are well overlaid with the

experimental data points as shown in **Figure 2**. Interestingly, the NRMSE values of Fluoxetine (0.41), Alprazolam (0.28), Quinidine (0.53), and Triazolam (0.29) are quite different, even though the simulated C-T curves of the four drugs are relatively satisfactory. Taken together, both the overlay of simulated C-T curves with the measured C-T data points and NRMSE should be used to evaluate the quality of the predicted ADME parameters by ADMET predictor. Overall, the predicted ADME parameters by ADMET Predictor can produce satisfactory C-T curves using SimCYP simulator for about half of the tested drugs.

Table 4 The comparison between predicted and observed PK profiles of all drugs

Drug name	Dosage	Pred/Obs	T _{Max} (h)	C _{Max} (ng/mL)	AUC (ng/mL·h)
Bupropion	150 mg	Pred	2.16	61.62	721.88
		Pred_v	1.86	71.84	614.66
		Obs[69]	(1.30, 5.10)	(34.00, 118.00)	(486.00, 1518.00)
Dextromethorphan	60 mg	Pred	1.56	13.13	195.70
		Pred_v	2.69	162.33	3594.67
		Obs[68]	NA	NA	NA
Bufuralol	15 mg	Pred	1.49	55.62	386.06
		Pred_v	1.75	18.66	151.83
		Obs[70]	(1.84, 2.74)	(56.00, 72.00)	(270.00, 430.00)
Quinidine	400 mg	Pred	1.16	1904.52	11632.95
		Pred_v	1.66	2183.40	18988.42
		Obs[71]	(0.36, 2.54)	(1330.00, 2070.00)	(3800.00, 14860.00)
Lorazepam	2 mg	Pred	1.92	18.24	240.28
		Pred_v	2.08	32.98	531.29
		Obs[67]	(0.50, 6.00)	(15.80, 25.60)	(197.20, 268.80)
Midazolam	7.5 mg	Pred	0.60	39.97	99.77
		Pred_v	0.87	39.58	383.67
		Obs[66]	(0.22, 1.21)	(25.90, 80.20)	(64.00, 163.70)
Alprazolam	0.8 mg	Pred	1.23	12.22	193.14
		Pred_v	2.16	7.74	327.10
		Obs[65]	(0.70, 2.30)	(8.20, 14.40)	(173.20, 291.60)

Table 4 (continued) The comparison between predicted and observed PK profiles of all drugs

Drug name	Dosage	Pred/Obs	T_{Max} (h)	C_{Max} (ng/mL)	AUC (ng/mL·h)
Triazolam	0.25 mg	Pred	0.72	2.34	13.94
		Pred_v	1.47	1.80	24.95
		Obs[64]	(0.35, 2.15)	(1.70, 4.30)	NA
Mephenytoin	100 mg	Pred	0.61	265.55	2576.76
		Pred_v	0.36	299.34	584.59
		Obs[63]	NA	NA	NA
Phenobarbital	216 mg	Pred	2.07	5235.78	660577.85
		Pred_v	4.03	4977.22	930922.01
		Obs[62]	2.00	5100.00	NA
Fluoxetine*	20 mg	Pred	4.36	6.50	186.21
		Pred_v	2.68	13.89	291.07
		Obs[43]	NA	NA	NA
Atomoxetine	20 mg	Pred	1.25	169.56	1390.42
		Pred_v	1.84	35.78	486.50
		Obs[61]	(0.50, 1.55)	(106.16, 178.16)	NA
Simvastatin	10 mg	Pred	1.20	2.11	7.03
		Pred_v	1.20	24.03	78.42
		Obs[60]	(1.00, 1.40)	(2.60, 4.60)	(7.40, 14.78)
Pravastatin	20 mg	Pred	0.96	40.60	130.36
		Pred_v	1.56	130.85	489.70
		Obs[60]	(1.00, 1.20)	(30.80, 42.20)	(92.00, 126.80)
Theophylline	100 mg	Pred	0.75	2589.22	29614.81
		Pred_v	0.62	1897.37	10003.06
		Obs[59]	(1.38, 1.82)	(1727.91, 2036.31)	(21499.55, 24439.65)
caffeine	100 mg	Pred	1.18	2540.84	13709.29
		Pred_v	1.50	2114.02	12859.90
		Obs[58]	(0.33, 2.00)	(1598.00, 2280.00)	(10700.00, 24438.00)
Imipramine	50 mg	Pred	3.03	25.37	250.72
		Pred_v	3.64	83.87	1082.01
		Obs[72]	(2.80, 3.80)	(20.90, 36.90)	NA
Desipramine	50 mg	Pred	5.42	13.56	264.97
		Pred_v	6.25	50.66	1042.14
		Obs[73]	(2.00, 10.00)	(12.1, 20.1)	(211.60, 413.20)

Pred: Predicted drug PK parameters from the unchanged SimCYP drug template (except Fluoxetine). Pred_v: Predicted drug PK parameters using SimCYP with input parameters from ADMET Predictor. Obs: drug PK parameter reported by clinical research. For Fluoxetine especially, the SimCYP drug template is modified to enable the predicted profile to fit the clinically reported curve.

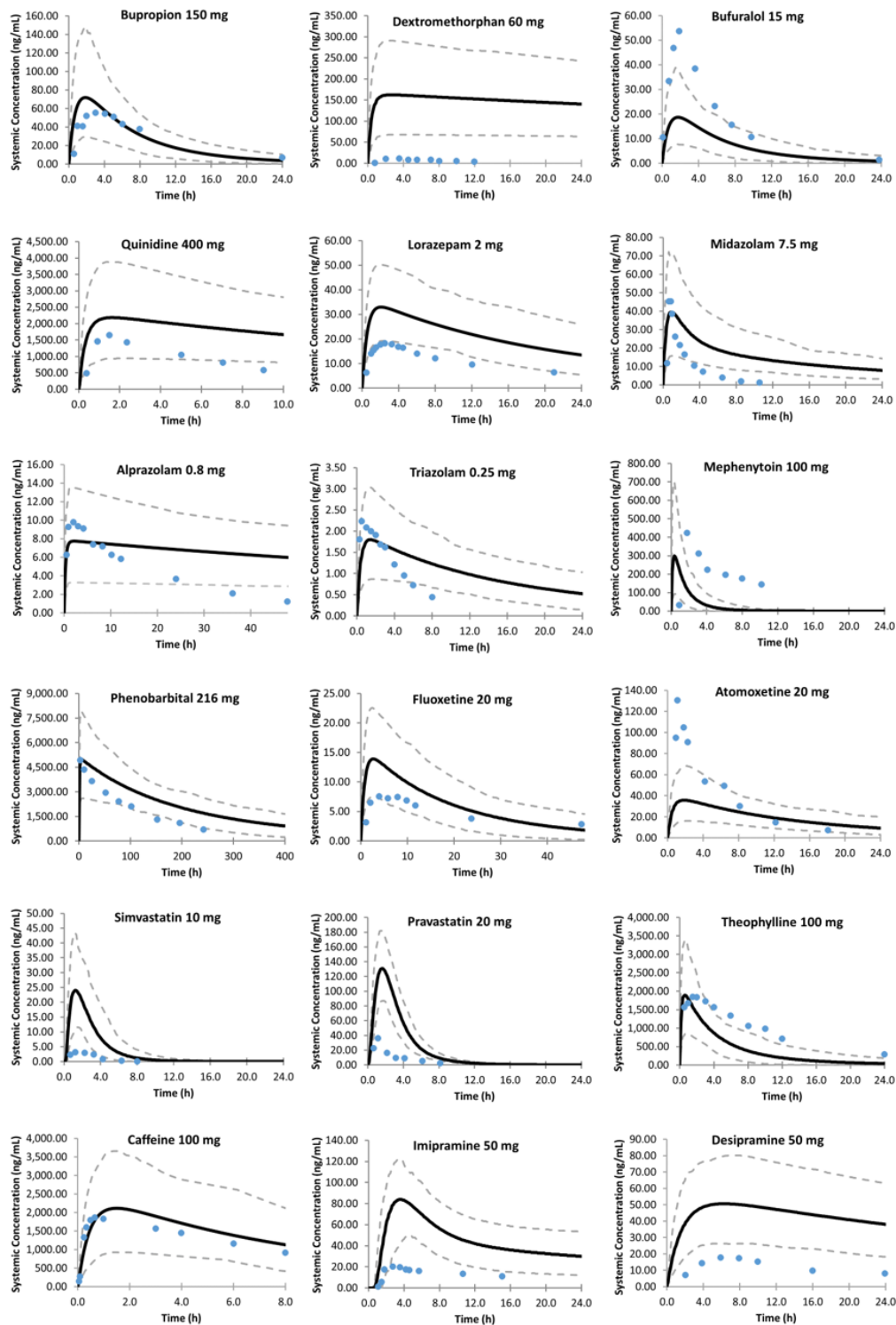


Figure 2 The predicted concentration profiles using SimCYP drug template with input parameters from ADMET Predictor and observed data of all drugs

Upper and lower dashed grey curves represent 95 % confidential interval

Table 5 Calculated NRMSE between predicted results by modified drug template and experimental concentration profiles of drugs

Name	NRMSE
Caffeine	0.13
Phenobarbital	0.22
Bupropion	0.26
Alprazolam	0.28
Theophylline	0.29
Triazolam	0.29
Midazolam	0.29
Bufuralol	0.36
Atomoxetine	0.40
Fluoxetine	0.41
Mephentyoin	0.48
Imipramine	0.51
Simvastatin	0.52
Pravastatin	0.53
Quinidine	0.53
Lorazepam	0.53
Desipramine	0.70
Dextromethorphan	0.93

3.1.3 Predicted concentration profiles for the in silico PBPK models

The C-T profiles predicted by all three versions (Versions 1, 2, and 3) of PBPK models are shown in **Figure 3**. The NRMSE value is also calculated to measure the difference between observed and predicted values of three versions respectively and summarized in **Table 5**. The table cell is colored in green if the NRMSE value of V1, V2, or V3 is lower than 0.2. In the following, we grouped all the 13 drug pairs / 26 drug pair sets into three groups according to their Tanimoto scores for the sake of discussion.

Group I ($TS \leq 0.7$). Six drug pairs, A-F, belong to this group. According to **Table 5**, the performance of the three protocols does not show an obvious pattern for Group I. The V1, V2 and V3 have two (A-1 and D-1), five (A-1, A-2, D-1, D-2 and F-1) and three (B-2, C-2 and D-2) pair

sets in green table cells, respectively. Most of those pair sets also exhibit a good overlay between experimental data points and prediction curves as shown in **Figure 3**, indicating the collaboration between SimCYP and ADMET Predictor is good. For the other groups from A-1 to F-2, all the three protocols have NRMSE values larger than 0.2 and the simulated C-T curves do not overlay with the experimental data points well. Interestingly, for D-2 drug pair set, though the NRMSE of the V2 model is the lowest, the predicted C-T curve by the V3 model has a better shape fitting the observed data as shown in **Figure 3**. This phenomenon is caused by the deviation of the first data point from the predicted curve of V3, which caused its NRMSE is larger than that of V2. When this outlier is eliminated and the NRMSE value is recalculated, V3 became the best for this pair set (NRMSE are now 0.57, 0.16 and 0.06 for the V1, V2 and V3 protocols, respectively).

Group II ($0.7 < TS \leq 0.9$). This group contains 5 drug pairs, G-K. As shown in **Table 6**, most drug pair sets have at least one version with an NRMSE value lower than 0.2, except H-1 and I-2. It is worthy to mention that the NRMSE value of I-2 is only 0.21 and the predicted C-T curve exhibits a good consistency with experimental data (**Figure 3**). The failure of H-1 model is likely caused by using problematic ADME parameters predicted by ADMET Predictor for the target drug. The “collaboration” between the two software should not be a problem for this drug pair since the NRMSE values of H-2 are very low for both the V2 and V3 models, which are 0.08 and 0.02 for the two models correspondingly. As shown in Table 6, the V3 version models apparently outperform the V1 and V2 models for most drug pair sets, as 7 out of 10 V3 models have NRMSE values lower than 0.2, while none of V1 models and 2 V2 models have their NRMSE values lower than 0.2. Interestingly, for drug pair set J-2, the V2 and V3 models have highly similar performance with good prediction result as shown in **Figure 3**; however, for K-2, all of the three

model versions do not exhibit satisfying prediction (**Figure 3**), even though the NRMSE values of the V1 and V2 models are equal to or lower than the cutoff.

Group III ($TS > 0.9$). This group contains 2 drug pairs, L and M. As shown in **Table 6**, most models have satisfactory NRMSE values. For L-1 and L-2 drug pair sets, the predicted profiles of the V2 and V3 models are very close to the clinical data points. Interestingly, for M-1 and M-2 drug pair sets, the performance of the V3 models is very poor. Drug pair M has a structural similarity with the Taminoto score of 0.95, interestingly, the V3 models perform poorly while the V1 and V2 models have not only satisfactory NRMSE values, but also very well-overlaid C-T curves with measured data points. This phenomenon may be explained by the prediction error by ADMET Predictor and error caused by the inherent difference between the two software can be compensated by the small difference of the ADME parameters between the template and target drugs. Indeed, the NRMSE values of the two drugs in drug pair M, 0.51 and 0.70, are very large (**Table 6**).

Table 6 Calculated NRMSE between predicted (three versions) and experimental concentration profiles of drugs in each group

Group-Drug	NRMSE (Different versions vs Obs)			Target drug NRMSE	Template drug NRMSE	Tanimoto score
	V1	V2	V3			
A-1	0.14	0.13	0.49	0.26	0.93	0.50
A-2	0.26	0.19	0.50	0.93	0.26	0.50
B-1	0.44	0.49	0.49	0.36	0.26	0.52
B-2	0.67	0.49	0.07	0.26	0.36	0.52
C-1	0.64	0.34	0.31	0.93	0.53	0.57
C-2	0.68	0.67	0.13	0.53	0.93	0.57
D-1	0.14	0.16	0.48	0.53	0.29	0.63
D-2	0.61	0.16	0.19	0.29	0.53	0.63
E-1	0.22	0.32	0.35	0.28	0.53	0.65
E-2	0.43	0.56	0.35	0.53	0.28	0.65
F-1	0.24	0.19	0.33	0.53	0.29	0.69
F-2	0.88	0.28	0.27	0.29	0.53	0.69
G-1	0.94	0.94	0.04	0.48	0.22	0.74
G-2	0.58	0.56	0.14	0.22	0.48	0.74
H-1	0.56	0.56	0.52	0.40	0.41	0.78
H-2	0.44	0.08	0.02	0.41	0.40	0.78
I-1	0.49	0.36	0.04	0.52	0.53	0.82
I-2	0.34	0.38	0.21	0.53	0.52	0.82
J-1	0.43	0.57	0.14	0.29	0.29	0.84
J-2	0.45	0.13	0.12	0.29	0.29	0.84
K-1	0.69	0.67	0.06	0.29	0.28	0.88
K-2	0.20	0.15	0.38	0.28	0.29	0.88
L-1	0.34	0.06	0.12	0.29	0.13	0.93
L-2	0.22	0.19	0.17	0.13	0.29	0.93
M-1	0.08	0.10	0.66	0.51	0.70	0.95
M-2	0.13	0.15	0.40	0.70	0.51	0.95

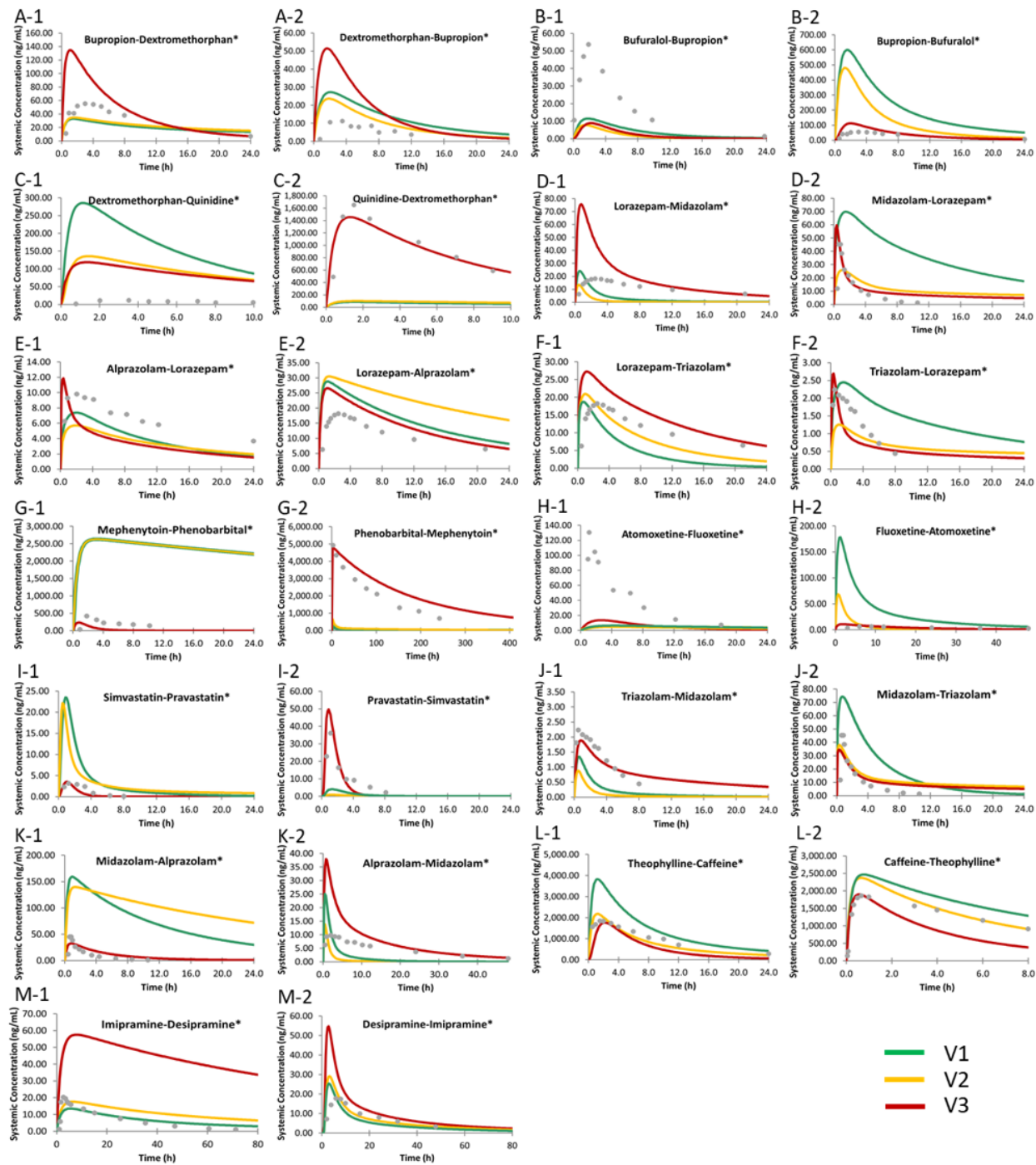


Figure 3 The predicted concentration profiles of three versions and observed data of all predicted drugs

Each template drug has a pound sign at the end.

3.2 PBPK Modeling for HCQ and optimized dosing regimens as a potential treatment for COVID-19

3.2.1 The PBPK model for HCQ

The PK profile predicted by the model we built for HCQ was shown in **Figure 4**. The simulated T_{Max} under 200 mg HCQ sulfate is 3.46 h, compared with FDA guidance of 3.26 h and literature report ranging from 2 - 4.5 h, respectively.[28,48,74] Simulated C_{Max} reported a value of 207.41 ng/ml, while the literature report C_{Max} is 188-427 ng/ml when the same dose was applied.[48] The clinical time-concentration profile of HCQ data was also extracted from literature and overlaid in **Figure 4**,[48] with all the data points located within the confidence intervals. The good alignment of our model and clinical data proves the reliability of our PBPK model.

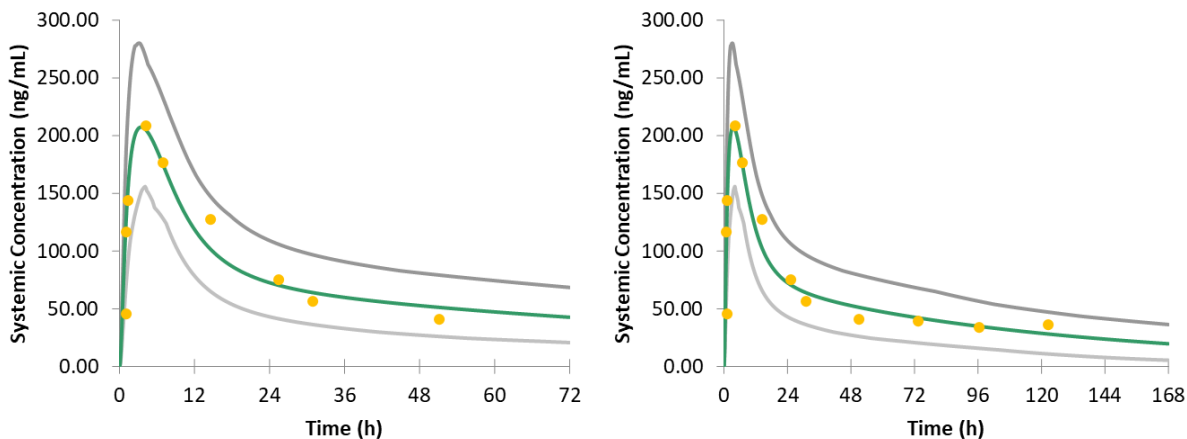


Figure 4 Validation of HCQ model within 3 days (left) and 7 days (right).

The green curve represents the mean value of the simulated virtual subjects and the grey curves represent the 90% confidence interval. The yellow dots represent the clinical reported 200 mg HCQ PK data

3.2.2 Simulation on different dosage regimens ranging from COVID treatment effective dose to cardiotoxicity dose

According to the FDA guidance and a series of clinical reports, dosage regimens ranging from 200mg, 400mg, 600mg, and 800mg multiple times a day. We first studied the drug plasma concentration fluctuation caused by different dosage regimens but the same total dosage amount, including 400 mg, 600 mg, and 800 mg within a day. As shown in **Figure 5**, under the circumstance of the same dosing load a day, multiple times of drug administration can help to maintain the stability of drug plasma concentration. From the peak concentration between one administration of the drug and the valley concentration before the next, the dosage regimen of 200mg TID shows the smallest drug plasma fluctuation, followed by 400mg BID. As a result, these dosing regimens are very suitable for maintaining the drug level after drug concentration has already reached the treatment level.

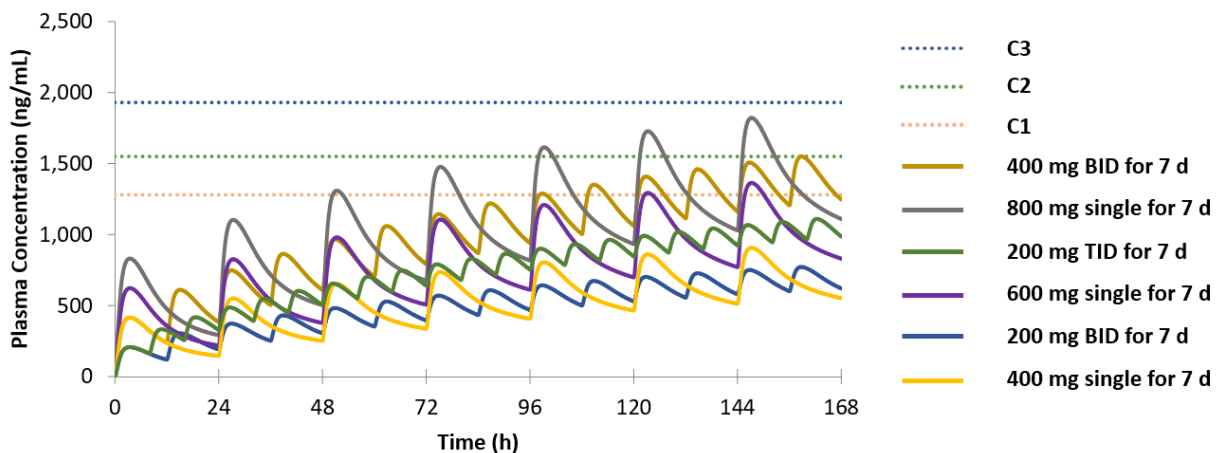


Figure 5 Drug plasma concentration under different dosage regimens, with each regimen colored with a different color

From most of the clinical data reported till now,[31-33,75-78] it is concluded that the treatment of more than 400 mg BID will show significant efficacy on the 5th day, while the

treatment of more than 600 mg BID for 5 to 7 days tends to result in the side effect of QT interval prolongation, which is the most important and severe side effect of this treatment. Continuous 800 mg BID is of high risk to cause severe cardiotoxicity during long-term treatment. Most clinical report with detailed evaluation for different dosage regimens lasts for 7 days. Since one aim of our study is to work out the optimized dose regimens, which is ensured with both treatment efficacy and circumvention of cardiotoxicity, we assumed that the peak blood concentration of 400 mg BID at the 5th day ($C1 = 1280$ ng/ml) is the value of the lowest effective dosing and the maximum concentration within 7 days ($C2 = 1550$ ng/ml) is that able to, in the most extent, avoid the significant QT interval prolongation. Meanwhile, the peak blood concentration for 600 mg BID treatment patients at the first-time drug administration on day 5 ($C3 = 1930$ ng/ml) is considered to be less safe but acceptable (**Figure 6**.) It is also shown that compared to lower dosing regimens, 600 mg BID can elevate drug plasma concentration to the level of $C1$ on the second day and $C2$ on the third day, while 800 mg BID enables drug plasma concentration to reach a level very close to $C1$ at the first day and exceed $C2$ at the second day. Thus, 600 mg BID and 800 mg BID serve as the beginning dose should help drug plasma concentration of patients reach effective treatment level faster than lower dosing regimens.

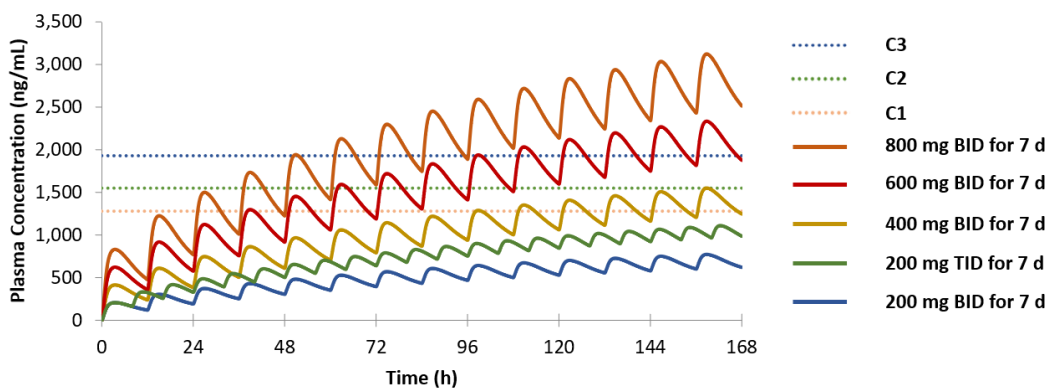


Figure 6 The predicted drug plasma C-T curved for a series of dosing regimens reported in clinical trials.

The horizontal dash lines represent the drug concentration level of $C1$, $C2$, and $C3$

3.2.3 Predicted PK profile for proposed dosing regimens

A series of dosing regimens designed have been shown in **Table 7**, using a higher dose as the beginning dose and a lower dose for maintaining plasma drug level. The simulation results of diverse dosing regimens are shown in **Figures 7 and 8**.

Table 7 A series of dosing regimens proposed in this study

	Day1	Day2	Day3	Day4	Day5	Day6	Day7	Recommended	
Regimen 1	600 mg BID	200 mg BID							
Regimen 2	600 mg BID		200 mg BID						
Regimen 3	600 mg BID	400 mg BID							
Regimen 4	600 mg BID		400 mg BID						A
Regimen 5	600 mg BID	200 mg TID							
Regimen 6	600 mg BID		200 mg TID						
Regimen 7	600 mg BID			200 mg BID					
Regimen 8	600 mg BID			400 mg BID					B
Regimen 9	800 mg BID	200 mg BID							
Regimen 10	800 mg BID		200 mg BID						
Regimen 11	800 mg BID	400 mg BID							
Regimen 12	800 mg BID		400 mg BID						D
Regimen 13	800 mg BID	200 mg TID							
Regimen 14	800 mg BID		200 mg TID						C
Regimen 15	800 mg BID		400 mg BID	200 mg TID					E
Regimen 16	800 mg BID		400 mg BID		200 mg TID				F

For each regimen, the same dose is represented by the same color, for example, 200 mg BID colored in light green is applied to Day2 to Day7 for Regimen 1.

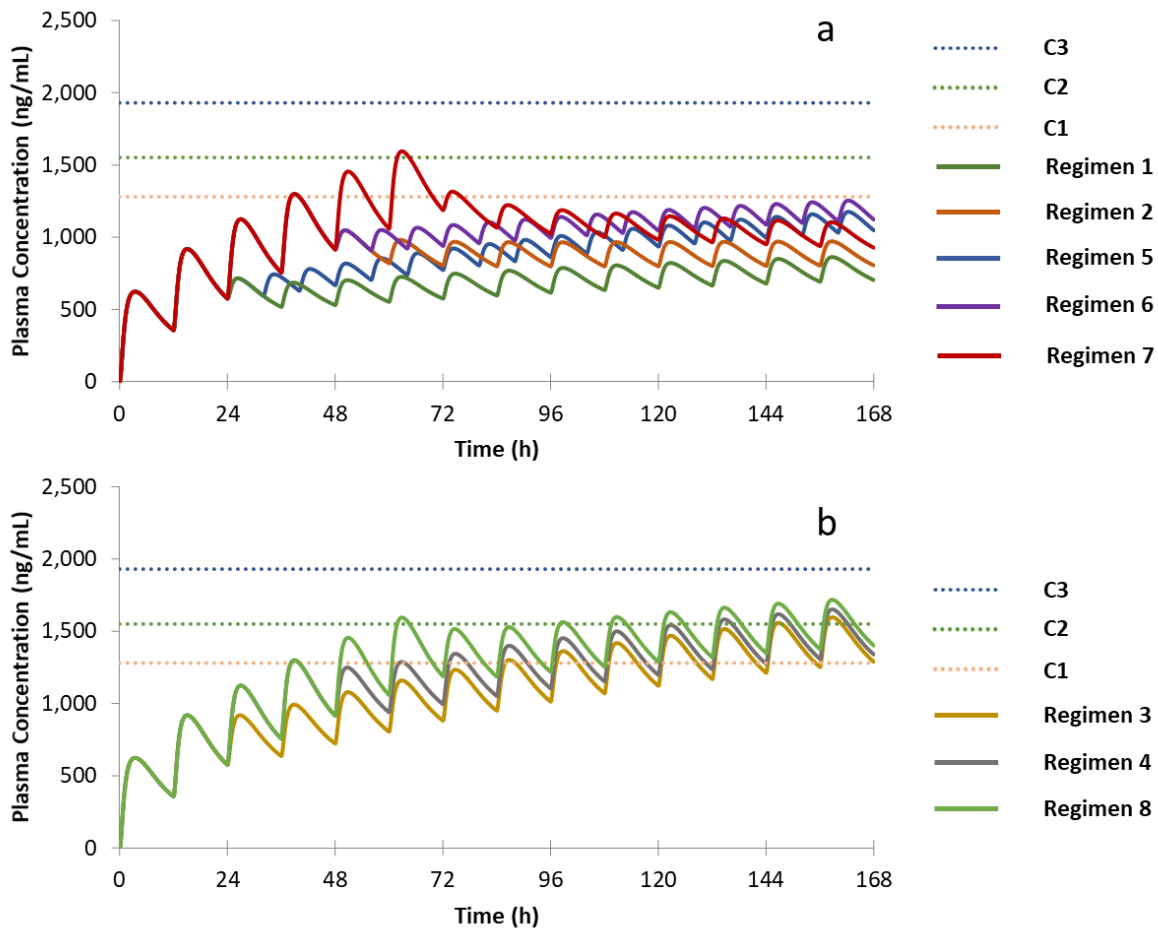


Figure 7 The time course of plasma drug concentration for Regimens 1-8 which administer 600 mg BID for first 1-3 days.

(a) Regimens 1, 2, 5, 6, and 7; (b) Regimens 3, 4, and 8

As shown in **Figure 7**, to start with 600 mg BID for the first two or three days (Regimens 2,4,6,7, and 8) is important for the drug plasma concentration to elevate rapidly at the beginning stage of drug treatment. For those dosage regimens, drug plasma levels can reach the C1 level on Day 2, while the drug plasma level reaches C1 on Day 5 for Regimen 3. Although the regimens of loading 600 mg BID on Day 1 and reduced dosage in the following days were (Regimens 1, 3, and 5) also proposed by some researchers, none of them can elevate drug plasma concentration to C1, the minimum effective drug plasma level, within the first three days. Thus, the administration of

600 mg BID for the first two or three days is strongly recommended. With regard to drug safety, Regimens 7 and 8, which administrate 600 mg BID for the first three days, drug plasma concentration can reach C2 on Day 3, but the maximum drug plasma level is still far below C3, the concentration at which significant QT interval prolongation may occur.

Interestingly, Regimens 2 and 6, which have doses of 600 mg BID for the first two days followed by doses of 200 mg BID or TID thereafter, cannot maintain the minimum effective treatment drug level after the first two days. Regimen 7, which applies 600 mg BID for the first three days followed by 200 mg TID afterward, cannot keep the plasma drug concentration within the effective treatment range either. On the contrary, the predicted curves of Regimens 4 and 8 show very promising results. With a starting dose of 600 mg BID for the first two or three days followed by 400 mg BID, drug plasma concentration can reach C1 on the second day and maintain a concentration level mainly between C1 and C2 in the following days. As soon as the two regimens are compared, Regimen 8 has slightly higher drug plasma concentrations than Regimen 4, is therefore more suitable for patients with much severer symptoms. It is pointed out that the maximum plasma concentrations of two regimens only slightly exceed C2, indicating their risk of causing cardiotoxicity is very low.

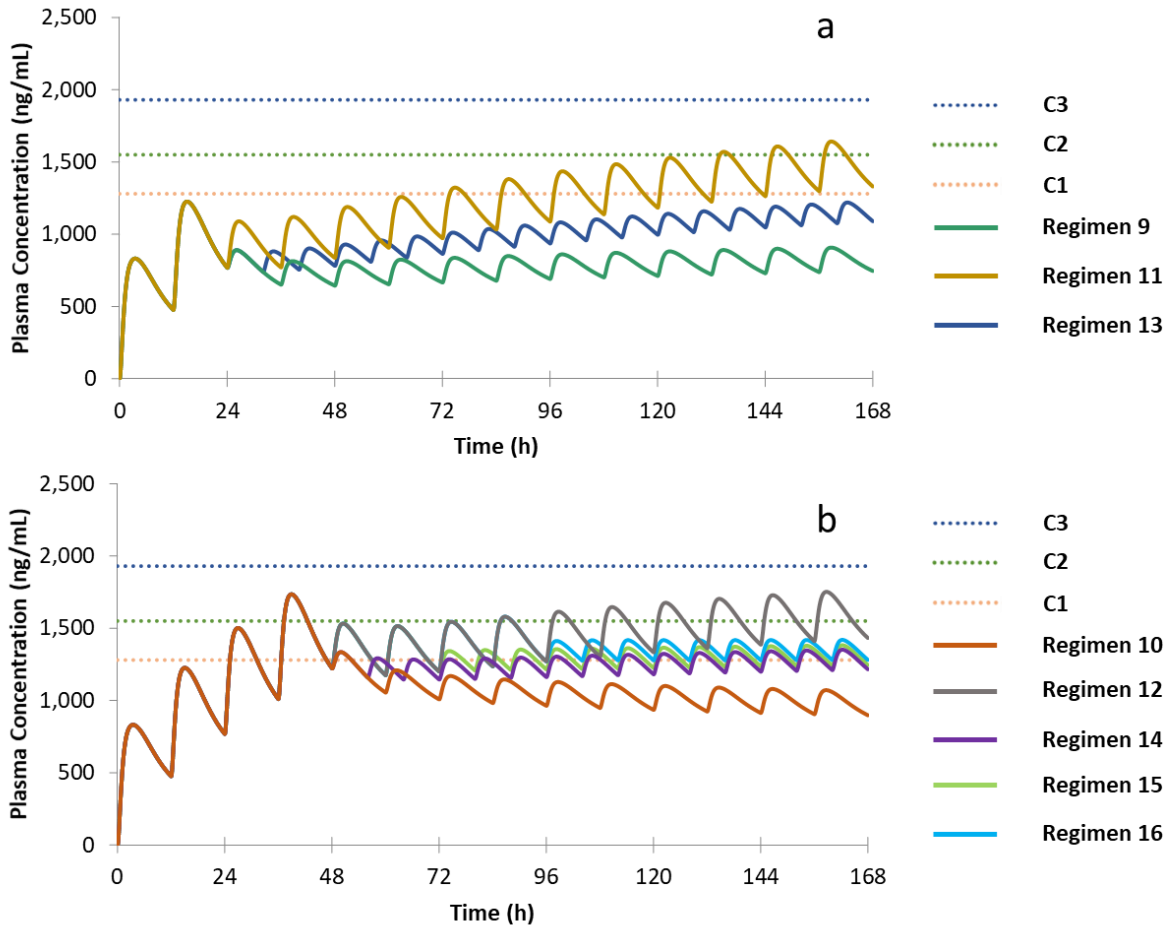


Figure 8 The time course of drug plasma concentration for Regimens 9-16 which administer 800 mg BID for first 1-3 days.

(a) Regimens 9, 11, and 13; (b) Regimens 10, 12, 14, 15, and 16

The time course of plasma concentration for dosing regimens starting with 800 mg BID were shown in **Figure 8**. Compared to the dosing regimens with starting doses of 600 mg BID on Day 1, starting doses of 800 mg BID can elevate drug plasma concentration close to C1 on the first day of the drug treatment. If the same doses are given in Day 2, the maximum concentration exceeds C2 in Day 2, and most plasma drug concentrations are between C1 and C2. In contrast, if lower doses are given in Day 2, as for Regimens 9, 11, and 13, the plasma drug concentrations cannot reach C1 level if the daily doses are only 200 mg BID or TID. Even daily doses of 400 mg

BID are administered (Regimen 11), the plasma drug concentrations cannot reach the effective treatment zone in the first three days.

As illustrated in **Figure 8b**, Regimens 12, 14, 15, and 16 have more promising C-T curves. All these drug regimens have 800mg BID on Day 2. For Regimen 16, the predicted drug plasma concentration is the highest among all the regimens. However, the peak values in this curve exceed the C2 multiple times, which may lead to a higher risk of causing severe cardio side effects. On the other hand, Regimen 10 is also problematic as the plasma drug concentration cannot reach C1 level after Day 2. Thus, Regimens 12, 14, and 15 are more appropriate to treat patients without severe symptoms. All the three regimens share very similar drug plasma concentration-time courses and the drug plasma concentration is well-maintained around C1 from Day 3 to Day 7.

3.2.4 Application of promising dosing regimens to special populations

We have selected six promising dosing regimens (**Table 7**) according to their time course of the plasma drug concentration. All the six regimens, Recommendations A to F, can well maintain their plasma drug concentration between C1 and C2 most time from Day 1 to Day 7. In the following, we conducted simulations for eight special populations. Moreover, the drug concentration-time courses in heart and lung were also predicted.

3.2.4.1 Recommendation A: Regimen 4 (600 mg BID for two days, followed by 400 mg BID)

As the C-T curves shown in **Figure 9**, the drug concentration levels are gradually elevated during the 7 days' treatment period for both the healthy volunteers and patients of special populations. The two renal impairment populations have extremely high drug concentrations in both blood and organs, followed by the elderly population and RA patients. Both renal impairment

populations and the elderly reach C3 on Day 4, indicating an increased risk leading to cardiotoxicity. The simulation curve of RA patients also shows an obvious elevation of drug concentration in both plasma and organs compared to healthy volunteers, but only occurs on Day 7. Thus, this regimen is acceptable for RA patients but not recommended. RA patients with heart diseases should better avoid this regimen. Pregnant and obese populations do not have much difference in plasma and organ concentration according to the simulation results, while pregnancy will lead to a little bit higher plasma and organ drug concentration. Overall, the C-T curves for Pregnant and obese subjects exhibit promising efficacy and acceptable risk from the prediction results, therefore, this dosing regimen might also be suitable for these two populations. Morbidly obese subjects tend to show no treatment effect as the predicted curve is below the C1 horizontal line during all the treatment periods. The predicted C_{Max} and T_{Max} during the first two days and the following 5 days are listed in **Table S4**.

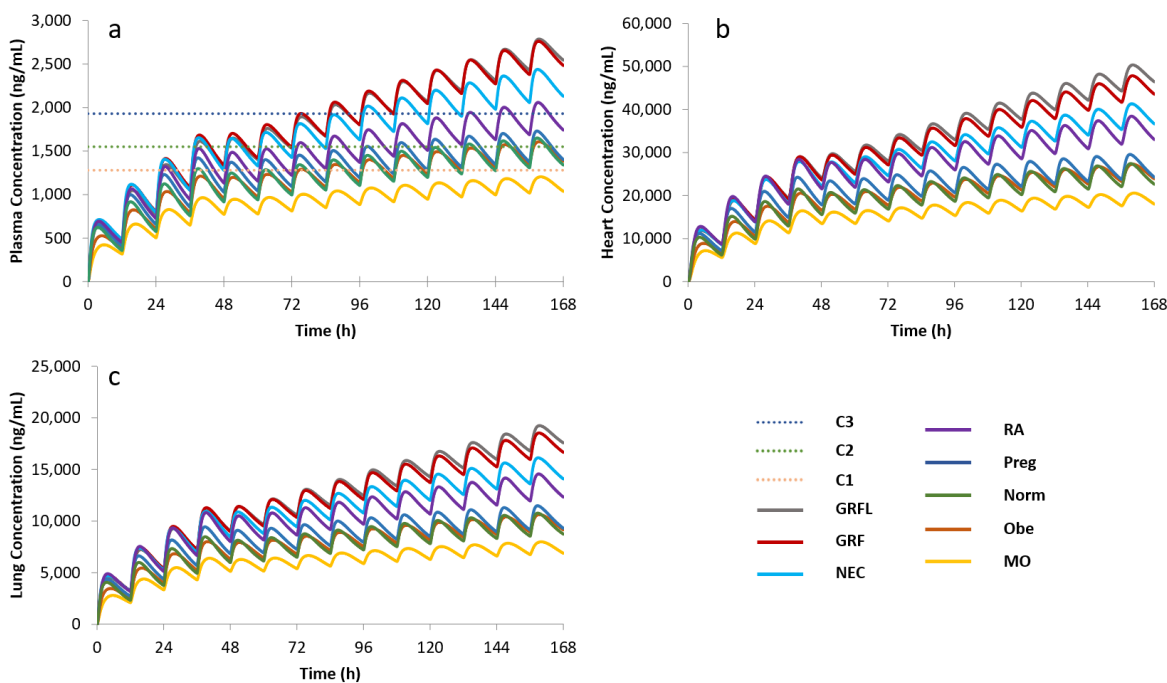


Figure 9 Predicted drug concentration profiles for different populations in plasma, heart, and lung under recommended dosing Regimen 4

3.2.4.2 Recommendation B: Regimen 8 (600 mg BID for three days, followed by 400 mg BID)

Similar to Regimen 4, drug plasma and organ concentrations during the first three days keep increasing and become more stable with a small growth, as shown in Figure 10 and listed in Table S5. Except for renal impaired subjects and elder subjects which still show a greatly elevated drug concentration in plasma and organs, the prolonged 600 mg BID dosing in Day 3 also results in the drug plasma concentration of RA patients reaching the C3 level one day earlier. Which is also similar to Regimen 4, pregnant and normal obese populations do not show an apparent difference compared to the simulation results of healthy volunteers, indicating this dosing regimen can be applied to these two populations. The predictive C-T curve of the morbidly obese population still shows a slightly lower concentration level but very close to C1. Therefore, Regimen 8 may be applicable to this population after a slight increase in the drug dose based on patients' weights.

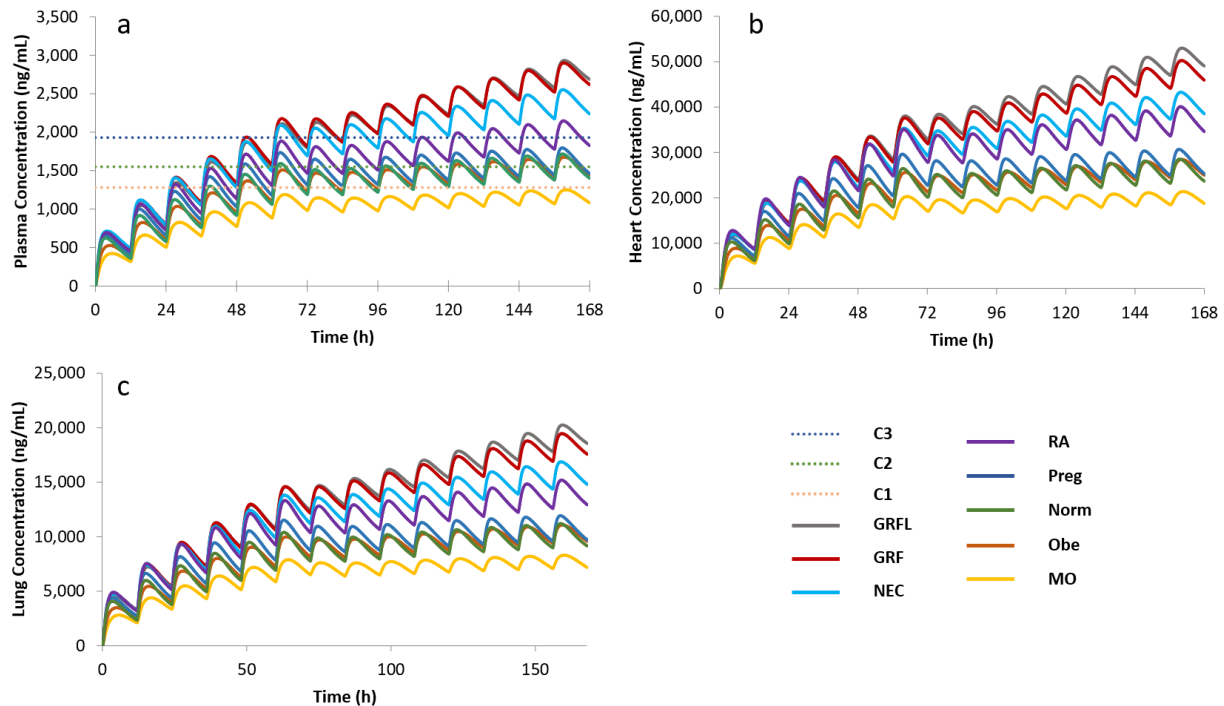


Figure 10 Predicted drug concentration profiles for different populations in plasma, heart, and lung under recommended dosing Regimen 8

3.2.4.3 Recommendation C: Regimen 14 (800 mg BID for two days, followed by 200 mg TID)

The simulation results for all the populations are shown in **Figure 11** and summarized in **Table S6**. The maximum drug concentrations in plasma and organs occur on Day 2 for all populations except for the two renal impairment populations for which the maximum drug concentrations occur on the last day of the treatment period. Similar to Regimens 4 and 8, the drug concentrations are above the C3 level in the last days of the treatment period. The C-T profile of Regimen 14 is more promising than Regimens 4 and 8 for the elder population as the plasma drug concentration only slightly exceed the C3 level only in the last two days. However, this regimen is not recommended for the elder population due to drug concentrations exceed the recommended

safety level. The drug plasma concentrations for the RA population are between C2 and C3. For other populations except for the morbidly obese population, the drug plasma concentrations are around C1 after Day 3. In summary, Regimen 14 may be applied to the RA, pregnant and obese populations, however, the patients' cardio condition should be carefully monitored when the maximum drug concentration occurs on Day 2.

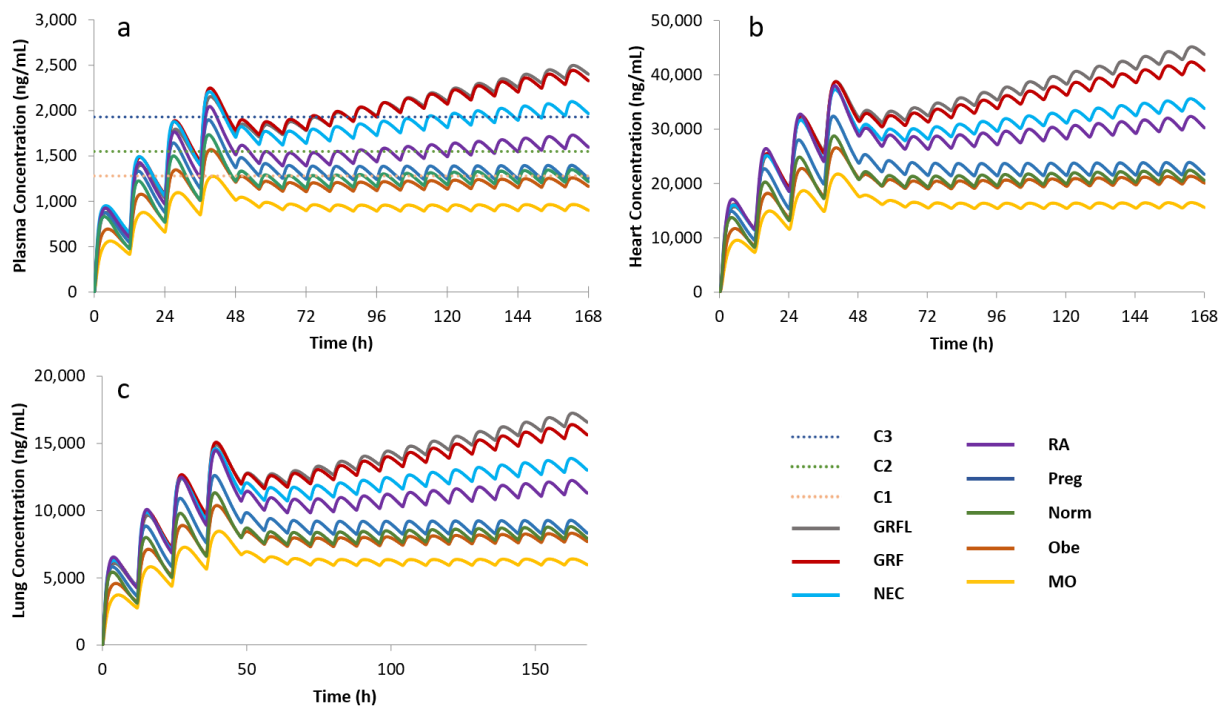


Figure 11 Predicted drug concentration profiles for different populations in plasma, heart, and lung under recommended dosing Regimen 14.

3.2.4.4 Recommendation D: Regimen 12 (800 mg BID for two days, followed by 400 mg BID)

The prediction results are shown in **Figure 12** and listed in **Table S7** for dosing Regimen 12 among different special populations. This regimen also shows impracticability for the two renal impairment populations and the elder population, as it has extremely high plasma and organ drug concentrations at the last stage of the treatment. The RA population also shows high drug

concentration in organs, with the predicted drug level being close to that of the elder population. For the pregnant population, the maximum drug concentration in plasma is between C2 and C3, a recommended concentration level when patients need a higher dosing regimen for treatment. The obese population has the simulation results showing the daily plasma drug concentration ranging between C1 and C2 since Day 2, revealing the promising treatment effect and dosing safety of this regimen for this population. Similarly, the predicted plasma drug concentration for the morbidly obese population is below but very close to C1. In summary, the pregnant, morbidly obese, and obese population show good stability during the drug concentration maintenance stage (from Day 3 to Day 7), suggesting that this regimen can be applied to these three populations. For the morbidly obese population, the dose may be slightly elevated based on a patient's body weight to achieve a better treatment effect.

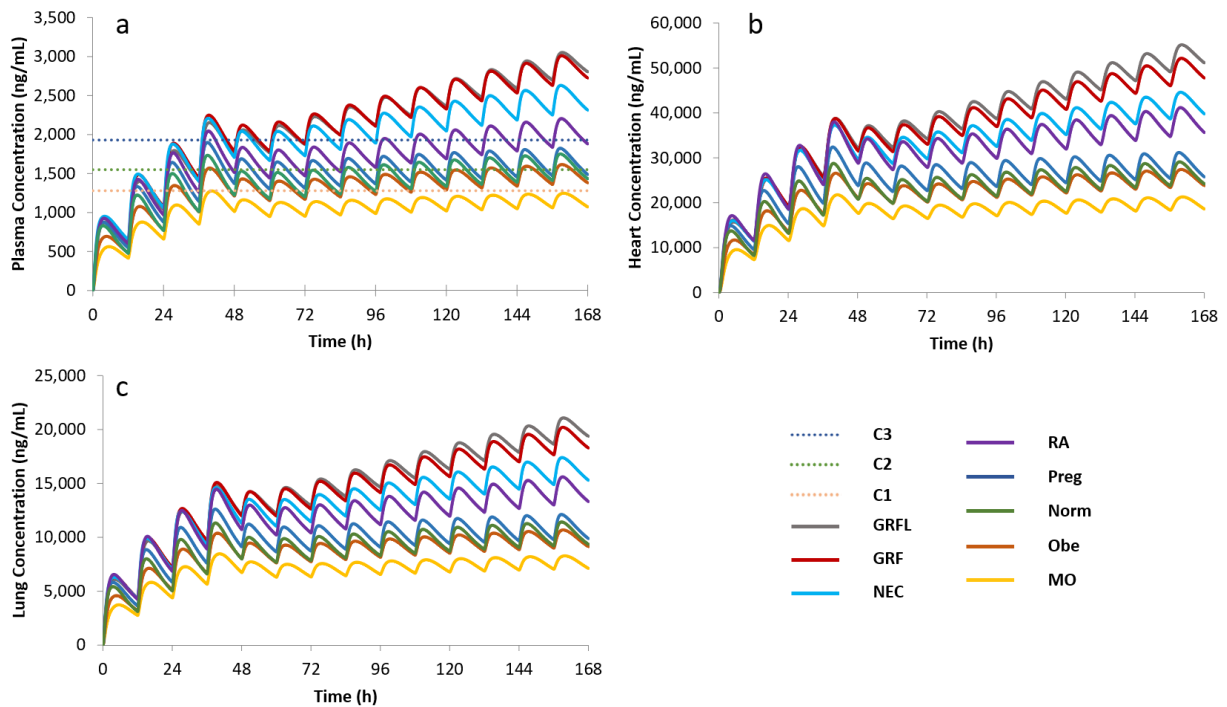


Figure 12 Predicted drug concentration profiles for different populations in plasma, heart, and lung under recommended dosing Regimen 12

3.2.4.5 Recommendation E: Regimen 15 (800 mg BID for two days + 400 mg BID for one days + 200 mg TID)

From the predicted C-T profiles shown in **Figure 13** and PK parameters summarized in **Table S8**, this regimen is still not recommended for the two renal impairment populations because of significant drug accumulation in plasma and organs. Most of the predicted curves for the elderly population and RA subjects reside between the C2 and C3 horizontal lines. Especially, considering that the elderly tend to have a cardiac problem and the predicted curve of the elder population is close to the C3 level, this dosing regimen is only recommended to elderly patients with severe symptoms. Unlike the plasma curves, the predicted organ concentrations for the elderly and PA populations are nearly the same (**Figure 13b and 13c**). For the pregnant population, the predicted drug concentrations in plasma and organs are slightly higher than obese and healthy populations in the first three days, but the drug levels are nearly the same since Day 4. Overall, this regimen has a similar characteristics as Regimen 12 (**Figure 12**) except that the stable drug concentrations are slightly lower. Thus, it may be used to treat pregnant women with mild symptoms. Last, the prediction results do not show a satisfying treatment effect for morbidly obese subjects.

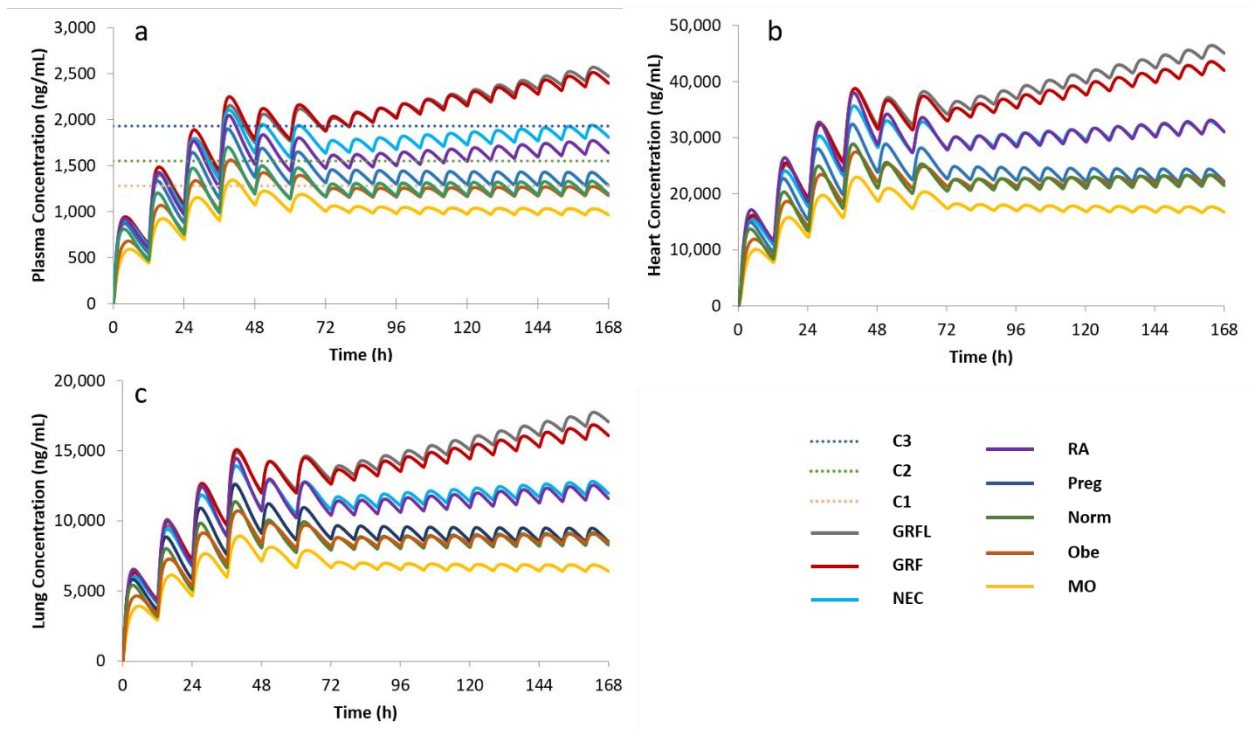


Figure 13 Predicted drug concentration profiles for different populations in plasma, heart, and lung under recommended dosing Regimen 15

3.2.4.6 Recommendation F: Regimen 16 (800 mg BID for two days + 400 mg BID for two days + 200 mg TID)

As shown in **Figure 14** and listed in **Table S9**, renal impairment and elder subjects have plasma drug concentrations exceed C3 since Day 2, indicating an extremely high risk of cardiotoxicity for the three populations. Other populations except for MO exhibit stable drug plasma and organ concentrations within both the effective treatment and safe ranges during the maintenance stage of the treatment period (the last five days). As to C_{Max} observed in Day 2, it is slightly higher than C3 for the RA population, a little bit lower than C3 for the pregnant populations. Compared to Regimen 15, the drug concentrations in both plasma and organs are

kept at a higher level since Day 4. Again, the predicted result is not likely to show treatment effect for the morbidly obese population.

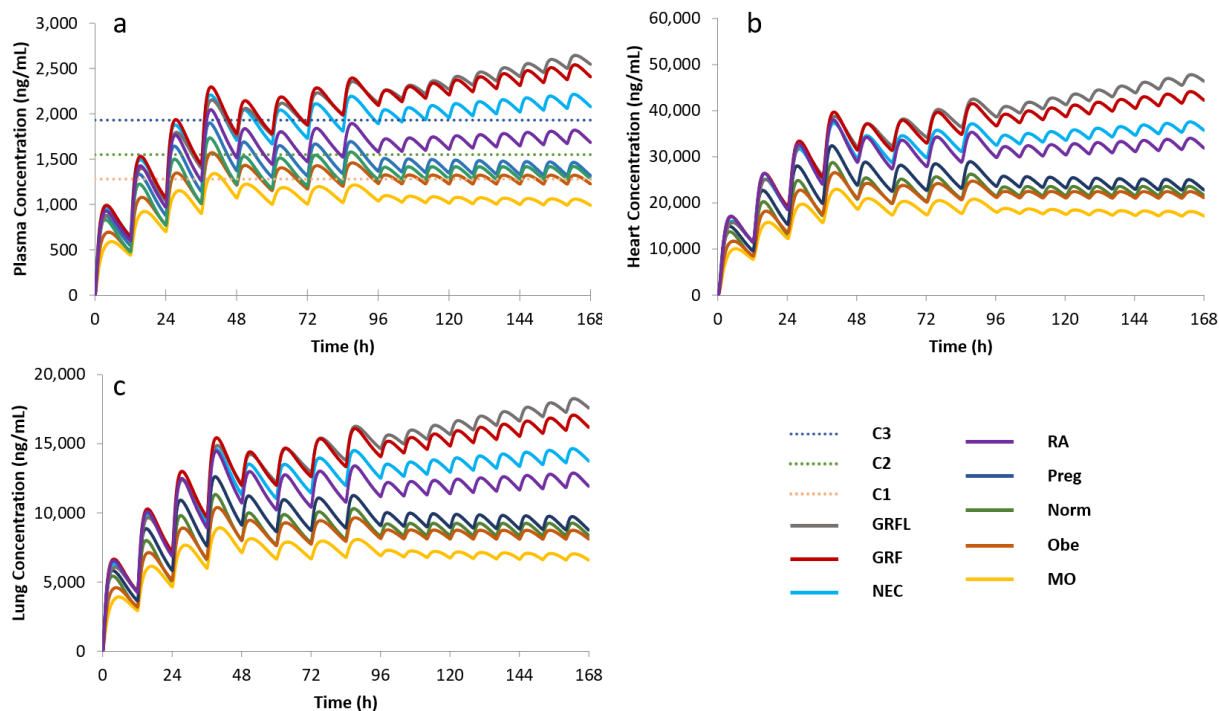


Figure 14 Predicted drug concentration profiles for different populations in plasma, heart, and lung under recommended dosing Regimen 16

3.2.4.7 Adjusted dosing regimens for renal impairment populations

The above-mentioned prediction results demonstrate that the renal impairment populations tend to have extensive drug accumulation in both plasma and organs especially in the treatment stage which aims to maintain stable drug concentrations. Thus, we ran simulations for the rest 10 regimens with smaller administrated dosage (Regimens 1, 2, 3, 5, 6, 7, 9, 10, 11, and 13), of which the prediction results are shown in **Figure S1** for GRF population and **Figure S2** for GRFL population. According to the curves of these dosing regimens, drug administration of 800 mg BID within one day (such as Regimens 10 and 13) or 600 mg BID on Days 1 & 2 (such as Regimens

2 and 7) can elevate drug plasma concentration to C2. Moreover, the administration of 800 mg drug in Day 1 (Regimen 10) and the administration of 600 mg drug in Days 1 & 2 (Regimens 2 and 7) exhibit a high probability of drug plasma concentration reaching and beyond C3. Moreover, the plasma concentrations are increased gradually after Day 2, suggesting a high cardiac risk to the renal impairment patients. Here we adjusted the dosing regimens with reduced dosages for the two renal impairment populations (**Table 8**). The predicted PK profiles are shown in **Figure 15** and PK parameters summarized in **Table S10**. The maintenance dose of 200 mg/day since Day 4 keeps the drug concentration in both plasma and organs around C1, successfully avoiding the consequence of increasing drug level in previously proposed regimens. Moreover, Regimen GR1 which begins with 600 mg BID is recommended to patients with cardio diseases or moderate symptoms, because the gradually elevated drug concentration enables the careful monitoring of side effects. On the contrary, Regimen GR2 which begins with 800 mg BID is more suitable for patients with severer conditions who urgently need rapidly increased drug concentration. The predicted curves for two renal impairment populations share a high similarity as illustrated in **Figure 15**.

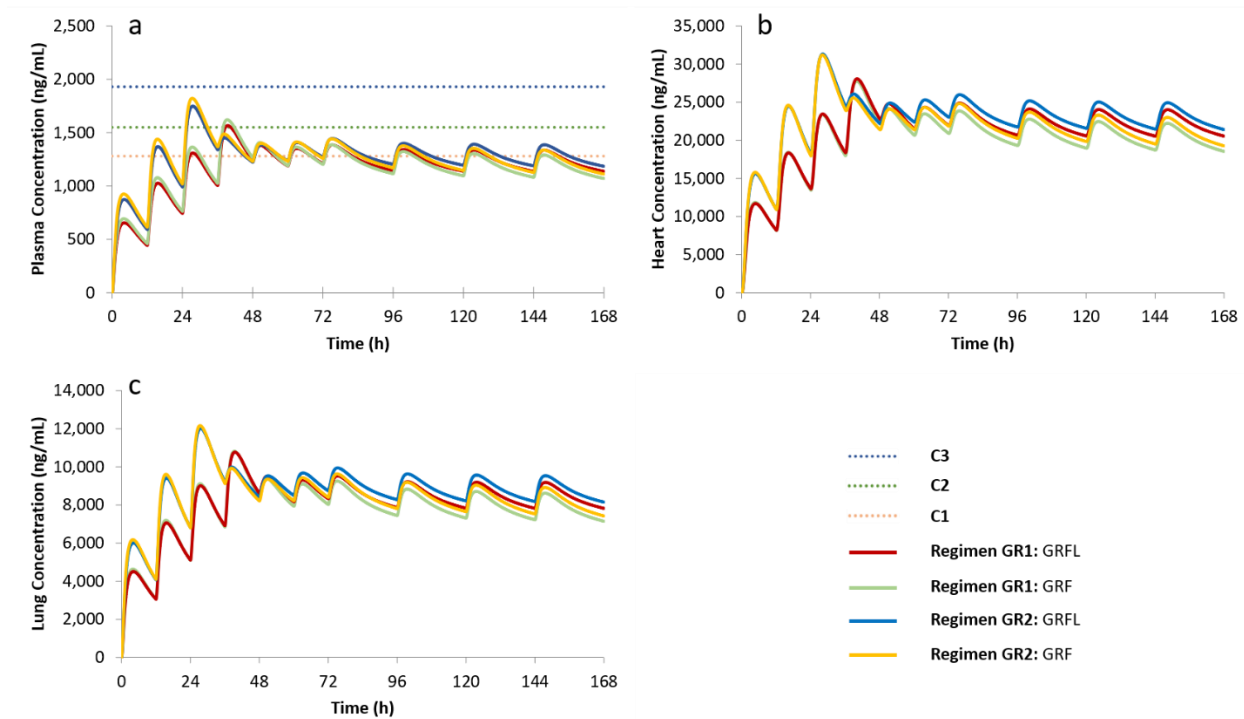


Figure 15 Predicted drug concentration profiles for two renal impairment populations in plasma, heart, and lung under two adjusted dosing regimens

Table 8 Regimens for the elder population and two renal impairment populations

	Day1	Day2	Day3	Day4	Day5	Day6	Day7
Regimen GR1	600 mg BID		200 mg BID	200 mg QD			
Regimen GR2	800 mg BID		200 mg BID	200 mg QD			
Regimen NR1	600 mg BID	400 mg BID					
Regimen NR2	600 mg BID		200 mg BID				
Regimen NR3	600 mg BID		200 mg BID				

↑
↑
 36h 72h

3.2.4.8 Adjusted dosing regimens for the elder population

Similar to the renal impairment population, the elder population also has more drug accumulation in both plasma and organs than the healthy population. As the simulation results are shown in **Figure S3**, 800 mg BID enables drug concentration to reach C2 in plasma on Day 2

(Regimen 10 and 13) while 600 mg BID for the first two days can elevate drug plasma concentration to C2 on Day 2 (Regimen 2 and 7), which is similar to the renal impairment population. However, the drug accumulation in the elder population is less severe compared to the renal impairment populations. Thus, two reduced dosing regimens are also proposed as listed in **Table 8**. The simulation results for the two revised regimens are shown in **Figure 16** and listed in **Table S11**. For the elder population, we not only minimized the cardiac risk by reducing dosages, but also shortened the duration of the first stage of the treatment so that drug concentration can reach effective treatment level rapidly. It is shown that all the three regimens, NR1, NR2 and NR3 have similar C-T profiles. NR1 and NR2 which start with 600 mg BID are recommended to elderly patients with cardiac diseases, while NR3 which begins with 800 mg BID at the first stage is recommended to patients with less severe COVID-19 symptoms.

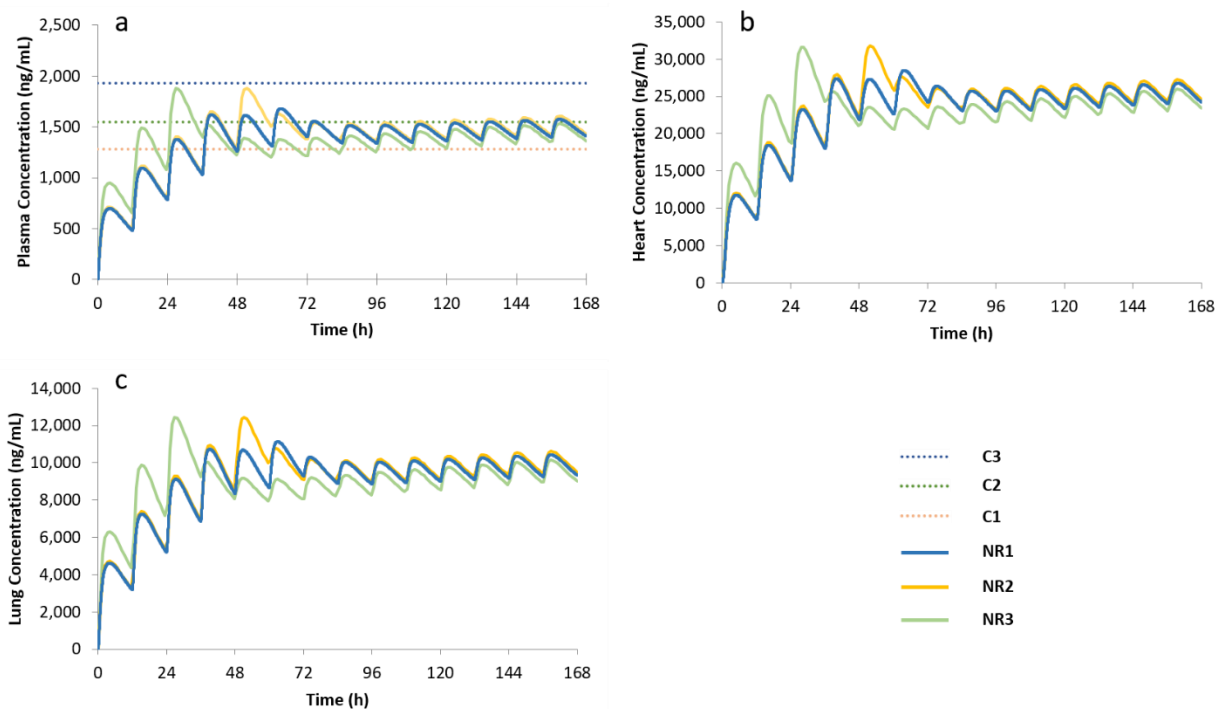


Figure 16 Predicted drug concentration profiles for the elder population in plasma, heart, and lung under two adjusted dosing regimens

4.0 Discussion

4.1 A New Approach for In Silico Prediction of Oral Drug Concentration Profiles in Human for Drug Candidates Lack Experimental Pharmacokinetic Data

In this study, we developed a novel approach to construct *in silico* PBPK models for target drugs lack experimental ADME and other PK parameters using an established PBPK model of a structurally similar drug as the model template. We used 18 drugs which formed 13 drug pairs (A-M) and 26 drug pair sets (each drug in a pair serves the template and target roles alternatively) to evaluate three ADME parameter substitution protocols, which are corresponding to three versions of PBPK models. The performance of the *in silico* PBPK models was critically evaluated using experimental PK profiles and parameters.

4.1.1 The practical guidance on selecting a suitable drug template

We attempted to obtain guidance on selecting a suitable template drug for a given target drug. We focused on using structural similarity to select the template drugs. It is found that drug pairs with Tanimoto score higher than 0.70 (Groups II and III) tend to show better predict performance among the three versions compared with drug pairs that with Tanimoto score lower than 0.70 (Group I). It is obvious that the higher structural similarity of two drugs within a drug pair should contribute to the higher possibility of good prediction results. After comparing the model performance of all three versions of models, we developed the following guidance: for Group I drug pairs, V2 or V3 is recommended; for Group II drug pairs, V3 is recommended; and

for Group III drug pairs, V2 is recommended. Following this practical guidance, 16 out of 26 drug pair sets have NRMSE values lower than 0.2, the threshold of recognizing a good PBPK model. Nevertheless, the prediction accuracy of ADMET Predictor and how much inherent difference between it and SimCYP are also very crucial factors that affect the model performance. From the evaluation of the error caused by combining the two software, the prediction accuracy of each modified drug template varied from each other, which shows the influence of the introduced error can have great difference for different drugs. Thus, the selection of substitution strategy should consider the NRMSE values of both template and target drugs. Unfortunately, in practice, only NRMSE of the template drug is known. An algorithm that can predict the NRMSE value of an arbitrary compound is therefore needed to further improve the practical guidance.

4.1.2 Another possible method to evaluate the prediction results of the three versions

There is also another method to evaluate the prediction results of V1, V2 and V3, which is the fold-error in the AUC of the three predict versions compared to the clinical data. However, the fold-error in the AUC can only show the difference between the total area under the prediction curve and the literature reported PK curve without delineating the concrete shapes of curves. On the contrary, the shape of the predicted drug C-T curve can be reflected by the difference between predicted and observed drug concentration at each time point when using RMSE as an evaluation method. Furthermore, the variation of the dosages can contribute to great RMSE discrepancy among drugs. For this reason, we normalized RMSE to eliminate the influence of dosages on RMSE value. The utilization of NRMSE can help to reduce the false-positive rate.

4.1.3 The perspective of applying *in silico* PBPK modeling for compounds lack experimental ADME and PK properties

SimCYP simulator is advanced software with well-constructed drug PK models in its built-in drug library, with each drug template containing comprehensive drug parameters. It can intuitively show simulated drug C-T curves contributed by these parameters under different trial designs. On the other hand, ADMET Predictor can predict a lot of PK parameters of an input compound based on its structural information without giving additional information. However, constructing a drug PK model needs full-scaled PK parameters and some of them cannot be predicted reasonably. Out of this consideration, we can partially rely on the PK parameters of another compound which shares high structural similarity with the unknown target compound. In this study, we put forward a novel approach to build PBPK models for a target drug which is in lack of measured ADME and other PK parameters using the PBPK model of a template drug which is structurally similar to the target drug. Also, we proposed overall guidance on selecting a suitable template drug and using its PBPK model as the model template. The success of this computational approach depends on two important factors, the availability of high quality PBPK model for the template compound and the accuracy and consistency of the ADME and PK parameters predicted by ADME Predictor software for the target drug. Thus, the performance of the two software can greatly contribute to the experiment results of our study. As a calculator of ADMET properties for compounds, the prediction results of drug properties may not be close enough to the real state, leading to errors when constructing drug models. Additionally, not all the ADME/PK properties can be calculated with the current version of ADME Predictor. For example, the prediction of metabolism in ADMET Predictor is only limited to 5 commonly used enzymes (CYP1A2, CYP2D6, CYP2C9, CYP2C19 and CYP3A4), and the prediction results of the transporters related

to the drug can only be reported qualitatively rather than quantitatively. On the other hand, there are currently 70 established compounds in SimCYP's drug libraries (including both the substrate library and the inhibitor library) and the libraries are still under development. We tested 18 compounds which shared structural similarity, and this study will replenish as more clinically validated PBPK models or related parameters for in-use drugs are available. Also, the utilization of Tanimoto score also has limitations. The calculated structural similarity between two compounds is based on smile strings, while not all structural components of a compound serve as functional parts. Weighted Tanimoto Coefficient for 3D structure similarity has been proposed by a study.[79] However, the weight allocation for different functional groups among compound series still needs further research.

Nevertheless, we have proposed a practical approach to generate PBPK models for a compound lack of experimental ADME/PK properties. This model can serve as the initial version of the PBPK models for the target compound, and its performance can be improved using the measured PK profiles and properties in the future. The computational protocol introduced in this work may have great applications in selecting drug leads to enter the drug optimization phase or drug candidates to enter preclinical studies.

4.2 Simulation on different dosage regimens ranging from COVID treatment effective dose to cardiotoxicity dose

In this study, the explored dosages include 200 mg, 400 mg, 600 mg, and 800 mg of HCQ by oral administration. This is because the most common available dosage form of HCQ is 200 mg HCQ sulfate (equivalent to 155 mg base). As an approved drug which is most commonly used

to treat Malaria and Rheumatoid Arthritis, the administration of a single-dose no larger than 800 mg is approved by FDA guidance.[80] To serve as a feasible treatment aiming at COVID-19, continuous dosage lower than 200 mg BID has been reported as no treatment effect, while 5 to 7 days' treatment dosing higher than 600 mg BID has been reported with a significantly improved treatment effect along with the elevated risk of QT prolongation side-effect. Especially, up to 5 days' treatment dosing of 800 mg BID was reported to have an extremely high risk to introduce QT-prolongation cardiotoxicity. During our research, we assumed that HCQ possesses treatment effect within therapeutic window according to its original treatment effect for other diseases and optimized dosing regimens to balance drug treatment efficacy and the risk of cardiac toxicity, and finally came out 6 recommended dosing regimens for normal patients. Based on the simulated C-T curves in plasma and lung and heart, we provided recommendations on dosage regimens for seven special populations.

Considering the situation that current hospital resources are in short, large amounts of patients will have to stay at home and follow the instructions of doctors instead of residing in hospitals to accept real-time monitoring and care. Thus, whether it is convenient for patients to follow doctors' directions is also taken into consideration during recommending dosing regimens to outpatients. Since taking medicine every eight hours a day is less practicable than taking medicines only twice a day for outpatients, regimens with 200 mg TID might not be suitable for them. On the contrary, in-hospital patients are more likely to have scheduled treatment on time. Thus, although Regimens 12, 15, and 16 have the maintenance dose of 200 mg TID at the end of the dosing schedule, it is still very practicable for in-hospital patients.

According to the prediction results for the two renal impairment populations and elder population, the drug accumulation in these subjects is much more significant than in healthy

subjects, resulting in an elevated drug level during the 7-day HCQ treatment period, which is very likely to cause severe side effects especially cardiotoxicity to patients. Thus, apart from the recommended 6 regimens, we specially design some reduced dosing regimens for those special populations. RA patients also have a higher accumulation of drugs compared to the healthy population. However, the predicted C-T curves of Regimen 15 for the RA population and the elder population are still below the C3 horizontal line and the drug levels in plasma and organs are well maintained during the 7-day treatment period. Interestingly, drug in the heart and lung tend to show more similar concentration level among RA patients and the elder population for different dosing regimens, although drug plasma concentrations of the elder population are always apparently higher than RA patients. It is reported that ABCB1 transporter, which is a key transporter of HCQ, was overexpressed on RA patients,[81] which means RA patients are more likely to suffer from cardiotoxicity side effects than the elder population under the same drug plasma level. The pregnancy and normal obese population only show a very small difference compared to healthy patients from the prediction results, and the drug concentration fluctuation pattern in both plasma and organs of these two special populations is very similar to that of the healthy population. For morbidly obese subjects, all the regimens recommended for the healthy population are unlikely to have a satisfactory treatment effect. Thus, it is recommended that the dosing level should be elevated based on their body weight when designing dosing regimens for this special population.

One thing that catches our attention is that the time for drug concentration peak in plasma is very close to that in lung. As a potential treatment targeting at COVID-19, the correlation between peak and valley of drug level in plasma and lung makes drug plasma concentration a fine indicator of drug lung concentration level. Another thing that also important is that the predicted

drug heart concentration is much higher than that in plasma. Although this is consistent with some literature reports that heart concentration of HCQ should be much higher than plasma drug level,[82] our PBPK model may not accurately predict the heart concentration. The PBPK model can be further improved by collecting more experimental PK and clinical data as well as measured PBPK parameters. For example, there are two main transporters, SLCO1A2 and ABCB1 for HCQ. [52,53] However, only the parameter of ABCB1 can be modified in SimCYP Simulator software. In addition, the measured parameters for CYP enzymes are also not available and we relied on the ADMET Predictor module in the Simulations-Plus software package to predict CYP parameters. Thus, the prediction precision of ADMET is also a key factor that affects the quality of our PBPK model for HCQ. For transporter parameters and blood binding parameters, we can only estimate the ranges for different parameters according to a variety of literature reports, and adjusting and compromising them to make predicted C-T curve be overlaid with clinical reported C-T profiles to the most extent. Moreover, the reliability of our prediction inevitably depends on the performance of the SimCYP software itself. Nevertheless, we tried to build a full PBPK model for HCQ to predict drug concentration in plasma, heart, and lung under different dosing regimens. Encouragingly, the predicted C-T curves can very well reproduce the measured plasma drug concentration at different time points as well as measured PK parameters. The importance of our work is not only to report possible drug levels in different organs for different populations, but also to design special population-dependent dosage regimens to maximize treatment effect and minimize possible cardiac toxicity at the same time. Although some difference between prediction and real circumstance exists, the simulation results can still uncover many mysteries during the clinical administration of HCQ as a treatment of COVID-19, which include the relationship of C-T profiles between different populations, the relationship of absorption and elimination lag time

between plasma and organs, and the fluctuation of organ drug level under different dosing regimens. Moreover, the sudden interest in HCQ has resulted in a shortage of treatment for its original aims, including malaria and autoimmune disease.[83] For individuals that lack practicable HCQ dosing regimens aiming at COVID-19, a treatment that well balances efficient treatment and safety must be found. Meanwhile, for those COVID-19 patients who may be suitable for HCQ treatment, we hope this study provides guidance on choosing suitable dosing regimens.

5.0 Conclusions

5.1 An approach to predict oral drug concentration profiles for drug candidates lack experimental PK data

In this work, we have introduced and tested a novel computational protocol to develop *in silico* PBPK model for a compound lack of measured ADME/PK properties and PK profiles. The general idea is to choose a proper PBPK model as the template, when the corresponding compound, the template drug, is structurally similar to the target drug. For the target drug, we calculated the ADME properties using ADMET Predictor of SimulationPlus. We have come out with an overall guidance using this method to build PBPK models for an arbitrary drug. First of all, the structural similarity between the template and the target drug is very important, thus template drugs which have the highest structural similarity to the target drug should be first considered; second, once the target drug is selected, the ADME parameter substitution protocol is selected based on the Tanimoto score (TS) between the target and template drugs. If TS is equal to or smaller than 0.7, V2 or V3 protocol is recommended; if TS is larger than 0.7 but smaller than or equal to 0.9, V3 protocol is suggested; and if TS is larger than 0.9, V2 is recommended. Following this guidance, more than 60% (16 out of 26) of the PBPK models have satisfactory performance. It is emphasized that this method highly relies on the collaboration between SimCYP and ADMET Predictor as well as the prediction accuracy of ADMET Predictor. The NRMSE values of the template and target drugs can guide us to select proper substitution protocol. If the NRMSE values are small, one can select a protocol with many ADME parameters being substituted, such as V3; however, if the NRMSE values are large, adopting V2 or V1 protocols

can minimize the error due to the poor “collaboration” between the two software. Unfortunately, the NRMSE value of the target drug is unknown in practice. A tool which can predict this NRMSE parameter is thus needed to further improve this method. While future experimental work is definitely needed to further improve the model performance, our novel approach proposed in this work can help identify drug candidates with favorable PK profiles, reducing experimental cost and providing insight in drug discovery and development.

5.2 PBPK modeling HCQ and proposed dosing regimens for healthy population and special populations as a potential treatment for COVID-19

In this study, we successfully constructed a PBPK model for HCQ which helps to predict drug PK profiles based on clinical PK information. A series of dosing regimens for the treatment of COVID-19 were designed and the time courses of drug concentrations in plasma and organs for both the healthy population and the special populations were predicted. Two regimens, one administrates 600 mg BID for the first two days followed by 400 mg BID (Regimen 4, Recommendation A) and the other administrates 600 mg BID for the first three days followed by 400 mg BID (Regimen 8, Recommendation B), are recommended to the healthy population, the pregnant population, and obese population, for which the drug concentration levels well fall within the effective treatment ranges and do not incur apparent cardiac toxicity. 800 mg BID for the first two days and 200 mg TID (Regimen 14, Recommendation C) is applicable to not only the healthy population, but also the RA, pregnant and obese populations. The maximum drug concentration during this regimen tends to appear on Day 2, which should be carefully monitored during the period. 800 mg BID for the first two days following by 400 mg BID (Regimen 12,

Recommendation D) can be considered by the healthy population, the pregnant population and the obese population. Regimen 15, which administrates drug 800 mg BID for the first two days, followed by 400 mg BID for one day, and 200 mg TID for the rest (Recommendation E) has the most versatile applicability, which can be considered by the elder population, RA population pregnant population, healthy population and obese population. however, the side effect caused by the drug regimen still needs carefully monitored on Day 2. Regimen 16 (Recommendation F) is similar to Regimen 15, but is not recommended for the elder population. The predicted drug plasma concentration of the morbidly obese population is always exhibiting little treat efficiency but good stability, which implies an increase of treatment dose based on a patient's body weight may be necessary to achieve better treatment effect. For the renal impairment population and elder population, we recommend the specially designed dosage regimens for them (Regimens GR1, GR2, NR1, NR2, and NR3) which not only achieves good treatment effect, but also avoids over-accumulation of drug in plasma and organs which increases the risk of HCQ treatment for COVID-19.

Appendix A Supplementary

Appendix A.1 Supplementary Tables

Table S1 Input parameters for 18 drugs (predicted by ADMET Predictor)

Drug name	Molecular Weight	Acidic pKa	Basic pKa	LogP	B/P	F _a
Alprazolam	308.772	None	3.01; 0.93; -0.62	2.629	0.781	9.271
Bufuralol	261.366	None	9.09	3.256	0.966	39.663
Bupropion	239.747	None	7.98	3.196	1.059	38.072
Caffeine	194.194	None	2.24	-0.153	1.08	83.508
Desipramine	266.389	None	9.67; 2.60	4.39	0.933	10.898
Dextromethorphan	271.405	None	8.91	3.806	1.096	26.993
Imipramine	280.416	None	8.96; 2.24	4.872	0.891	9.584
Lorazepam	321.164	11.16	1.61	2.361	0.789	9.533
Mephenytoin	218.257	11.32	None	1.423	0.825	42.713
Midazolam	325.775	None	4.57; 0.84	3.563	0.782	6.613
Pravastatin	424.538	4.92	None	2.184	0.662	9.645
Quinidine	324.425	None	7.95; 3.87	2.653	0.892	26.042
Simvastatin	418.577	None	None	4.981	0.76	8.237
Theophylline	180.167	9.36	2.11	-0.138	1.088	82.434
Triazolam	343.217	None	2.85; 0.87; -0.90	3.142	0.77	7.565
Phenobarbital	232.24	11.19; 7.58	None	1.628	0.763	21.378
Atomoxetine	255.362	None	9.72	3.766	0.87	19.76
Fluoxetine*	309.333	None	9.82	4.388	0.882	15.89

Table S1 (Continued). Input parameters for 18 drugs (predicted by ADMET Predictor)

Drug name	ADME					
	V _{ss}	P _{eff} (cm/s·10 ⁴)	CYP1A2		CYP2C9	
			K _m (μM)	V _{max} (nmol/min/ nmol)	K _m (μM)	V _{max} (nmol/min/ nmol)
Alprazolam	1.386	5.519	7.194	1.128	12.44	0.125
Bufuralol	3.196	2.15	56.575	69.834	43.441	15.42
Bupropion	5.212	4.209	29.549	57.021	37.056	16
Caffeine	0.511	4.013	43.551	0.792	15287	0.757
Desipramine	9.332	4.288	183.854	10.225	46.471	0.56
Dextromethorphan	4.691	5.037	NonSubstrate	NonSubstrate	NonSubstrate	NonSubstrate
Imipramine	9.578	5.423	239.273	18.989	26.007	0.216
Lorazepam	0.804	4.015	NonSubstrate	NonSubstrate	10.637	0.588
Mephentoin	0.979	3.803	114.202	318.486	339.284	0.264
Midazolam	1.861	7.545	6.206	1.235	3.376	0.157
Pravastatin	0.299	1.068	NonSubstrate	NonSubstrate	30.616	3.361
Quinidine	2.258	2.209	NonSubstrate	NonSubstrate	19.873	1.352
Simvastatin	0.815	3.832	NonSubstrate	NonSubstrate	NonSubstrate	NonSubstrate
Theophylline	0.542	2.927	155.108	2.753	22167.33	1.797
Triazolam	1.451	6.125	9.895	1.567	5.843	0.136
Phenobarbital	0.642	2.554	NonSubstrate	NonSubstrate	536.686	0.652
Atomoxetine	4.783	4.194	12.552	4.879	31.643	32.1
Fluoxetine	10.662	2.707	NonSubstrate	NonSubstrate	14.75	15.112

Table S1 (Continued). Input parameters for 18 drugs (predicted by ADMET Predictor)

Drug name	ADME					
	CYP2C19		CYP2D6		CYP3A4	
	K_m (μ M)	V_{max} (nmol/min/nmol)	K_m (μ M)	V_{max} (nmol/min/nmol)	K_m (μ M)	V_{max} (nmol/min/nmol)
Alprazolam	53.743	0.517	NonSubstrate	NonSubstrate	72.727	7.186
Bufuralol	26.629	45.725	3.196	4.816	NonSubstrate	NonSubstrate
Bupropion	32.699	171.573	1.247	0.128	554.231	0.786
Caffeine	967.276	1.584	NonSubstrate	NonSubstrate	191.235	1.809
Desipramine	47.202	92.572	2.977	22.246	47.667	2.676
Dextromethorphan	9.964	10.616	11.393	14.084	64.946	4.797
Imipramine	39.11	20.748	14.145	19.579	68.448	5.232
Lorazepam	NonSubstrate	NonSubstrate	NonSubstrate	NonSubstrate	114.62	6.113
Mephenytoin	52.298	0.943	219.547	1.595	255.08	9.131
Midazolam	37.194	0.445	NonSubstrate	NonSubstrate	46.268	8.63
Pravastatin	NonSubstrate	NonSubstrate	NonSubstrate	NonSubstrate	NonSubstrate	NonSubstrate
Quinidine	NonSubstrate	NonSubstrate	30.321	6.922	79.661	12.611
Simvastatin	NonSubstrate	NonSubstrate	NonSubstrate	NonSubstrate	1.86	2.577
Theophylline	NonSubstrate	NonSubstrate	NonSubstrate	NonSubstrate	157.732	2.632
Triazolam	NonSubstrate	NonSubstrate	NonSubstrate	NonSubstrate	63.494	5.927
Phenobarbital	54.67	0.493	NonSubstrate	NonSubstrate	NonSubstrate	NonSubstrate
Atomoxetine	83.696	122.706	1.02	12.218	126.224	6.291
Fluoxetine	32.43	59.172	0.468	1.459	144.748	9.54

All the parameters for Fluoxetine were input to build its adjusted template model. When serving as the target drug, Atomoxetine was predicted based on the adjusted Fluoxetine template.

Table S2 Modified parameters predicted by ADMET Predictor for Fluoxetine template.

Parameter	Input Value
Physiochemical Properties	
LogP	4.05*
pKa	9.82 (Monoprotic Base)**
Blood Binding	
B/P	0.94*
F _u	0.1589**
Absorption (ADAM model)	
P _{eff} (10 ⁻⁴ cm/s)	2.707**
Distribution (Full PBPK model)	
V _{ss} (L/kg)	20*
Elimination	
CYP2C9	V _{max} : 15.112, K _m : 14.75**
CYP2C19	V _{max} : 59.172, k _m : 32.43**
CYP2D6	V _{max} : 1.459, K _m : 0.468**
CYP3A4	V _{max} : 9.54, k _m : 144.748**

B/P: blood-to-plasma partition ratio. F_u: the fraction of unbound drug in plasma. P_{eff}: human jejunum effective permeability. V_{ss}: volume of distribution at steady state using tissue volumes for a population representative of healthy volunteer population. V_{max}: maximum rate of metabolism (pmol/min/pmol of isoform). K_m: Michaelis-Menten constant, (μM). *: data from DrugBank. **: ADMET Predictor prediction result.

Table S3 Predicted PK parameters by SimCYP Simulator of each group.

	V1			V2			V3		
	T _{Max} (h)	C _{Max} (ng/mL)	AUC (ng/mL.h)	T _{Max} (h)	C _{Max} (ng/mL)	AUC (ng/mL.h)	T _{Max} (h)	C _{Max} (ng/mL)	AUC (ng/mL.h)
A-1	1.56	32.83	489.24	1.57	34.70	543.78	1.09	134.80	1029.77
A-2	2.05	27.26	301.76	1.92	23.64	220.52	1.69	51.44	368.52
B-1	1.81	11.50	90.49	1.45	7.78	41.83	2.16	8.89	52.77
B-2	1.56	599.76	4987.74	1.20	480.26	2894.68	2.04	111.93	902.70
C-1	1.16	285.58	1745.00	1.43	135.74	997.00	1.31	118.71	907.86
C-2	1.50	84.44	673.03	1.70	102.08	861.95	1.28	1455.19	9744.15
D-1	0.60	24.14	73.21	0.48	13.52	25.17	0.77	75.75	447.09
D-2	1.56	69.79	903.96	1.09	25.88	267.20	0.37	59.60	228.05
E-1	1.92	7.39	115.82	1.92	5.72	113.98	0.36	11.88	82.52
E-2	1.13	28.82	391.50	1.33	30.50	541.49	1.13	26.58	342.62
F-1	0.72	18.73	112.33	0.96	20.96	187.37	1.20	27.27	340.55
F-2	1.56	2.45	33.74	1.08	1.26	15.46	0.37	2.69	13.64
G-1	3.17	2629.04	57296.38	3.17	2629.02	57294.61	0.74	235.49	620.85
G-2	2.06	352.27	11977.41	2.07	655.13	29764.21	2.06	4833.39	847522.37
H-1	4.34	6.51	121.20	4.23	5.64	103.68	2.52	13.66	130.62
H-2	1.25	178.63	1565.18	0.72	68.62	234.49	1.72	10.84	189.81
I-1	0.84	23.50	69.71	0.48	22.17	67.13	1.08	3.51	7.11
I-2	1.33	4.01	14.42	1.32	0.88	2.99	0.88	49.64	87.57
J-1	0.63	1.35	4.17	0.50	0.88	1.81	0.86	1.89	17.23
J-2	0.72	74.37	421.55	0.37	38.06	272.29	0.37	34.57	226.19
K-1	0.98	159.28	1845.88	1.33	139.77	2466.26	0.89	32.66	194.88
K-2	0.50	25.10	73.42	0.50	13.87	25.13	0.77	37.94	354.16
L-1	1.24	3822.30	33567.68	1.23	2180.61	18538.33	2.16	1768.43	13202.95
L-2	0.75	2468.92	14595.42	0.64	2374.07	12320.61	0.56	1898.85	7753.21
M-1	5.62	13.53	550.05	6.43	17.61	896.25	8.03	57.56	3596.48
M-2	2.83	25.33	380.99	3.23	29.20	490.96	2.83	54.77	776.18

Table S4 The predicted maximum drug concentration and the corresponding time during two dosing periods of dosing regimen 4

Day1-day2						
	Plasma		Heart		Lung	
	Time	Concentration	Time	Concentration	Time	Concentration
GRF	39.41	1685.07	40.32	29041.93	39.41	11306.71
GRFL	39.58	1613.70	40.42	29047.19	39.61	11146.25
MO	40.52	965.84	41.19	16485.73	40.52	6414.31
NEC	39.11	1654.06	40.12	27936.67	39.14	10947.48
Obe	39.78	1212.68	40.59	20563.74	39.82	8025.06
Preg	38.88	1422.82	39.45	24277.97	38.88	9454.71
RA	39.25	1531.09	39.95	28453.55	39.28	10831.63
	38.94	1299.25	39.68	21551.62	38.94	8490.04

Day3-day7						
	Plasma		Heart		Lung	
	Time	Concentration	Time	Concentration	Time	Concentration
GRF	159.23	2763.04	160.10	47857.05	159.23	18540.60
GRFL	159.40	2787.99	160.24	50367.36	159.43	19253.22
MO	160.04	1205.13	160.74	20591.75	160.07	8001.40
NEC	158.89	2439.52	159.84	41349.35	158.93	16136.77
Obe	159.40	1608.47	160.21	27324.13	159.40	10643.39
Preg	158.69	1731.06	159.23	29580.97	158.69	11500.58
RA	159.10	2059.87	159.80	38455.56	159.10	14578.19
Norm	158.76	1651.28	159.50	27448.87	158.76	10779.77

GRF: renal impairment population, 30 mL/min≤GRF≤60 mL/min, GRFL: renal impairment population, GRF≤30 mL/min, MO: morbidly obese population, NEC: geriatric Northern European Caucasians population, Obe: obese population, Preg: pregnant population, RA: rheumatoid arthritis population and Norm: healthy volunteers.

Table S5 The predicted maximum drug concentration and the corresponding time during two dosing periods of dosing regimen 8

Day1-day3						
	Plasma		Heart		Lung	
	Time	Concentration	Time	Concentration	Time	Concentration
GRF	63.37	2177.50	64.28	37600.27	63.37	14611.64
GRFL	63.54	2111.53	64.38	38064.00	63.57	14584.72
MO	64.38	1189.75	65.05	20318.28	64.38	7901.16
NEC	63.07	2090.42	64.04	35356.76	63.07	13833.67
Obe	63.67	1510.47	64.48	25633.00	63.71	9995.95
Preg	62.83	1736.42	63.37	29648.63	62.83	11538.40
RA	63.20	1885.74	63.91	35100.19	63.24	13341.96
Norm	62.90	1594.45	63.64	26473.98	62.90	10416.37
Day4-day7						
	Plasma		Heart		Lung	
	Time	Concentration	Time	Concentration	Time	Concentration
GRF	159.20	2902.85	160.10	50287.19	159.23	19478.78
GRFL	159.40	2934.09	160.24	53013.31	159.40	20262.18
MO	160.00	1252.50	160.68	21402.10	160.00	8315.83
NEC	158.89	2553.73	159.84	43291.39	158.89	16891.93
Obe	159.37	1676.43	160.17	28480.92	159.40	11093.09
Preg	158.66	1797.05	159.23	30710.85	158.69	11938.90
RA	159.10	2148.71	159.77	40122.27	159.10	15207.35
Norm	158.76	1717.85	159.47	28558.10	158.76	11213.89

GRF: renal impairment population, $30 \text{ mL/min} \leq \text{GRF} \leq 60 \text{ mL/min}$, GRFL: renal impairment population, $\text{GRF} \leq 30 \text{ mL/min}$, MO: morbidly obese population, NEC: geriatric Northern European Caucasians population, Obe: obese population, Preg: pregnant population, RA: rheumatoid arthritis population and Norm: healthy volunteers.

Table S6 The predicted maximum drug concentration and the corresponding time during two dosing periods of dosing regimen 14

Day1-day2						
	Plasma		Heart		Lung	
	Time	Concentration	Time	Concentration	Time	Concentration
GRF	39.41	2249.67	40.32	38773.87	39.45	15095.14
GRFL	39.58	2154.68	40.46	38786.24	39.62	14883.00
MO	40.39	1277.36	41.06	21781.90	40.39	8479.04
NEC	39.11	2208.87	40.12	37308.93	39.14	14619.62
Obe	39.65	1571.62	40.46	26590.57	39.68	10391.02
Preg	38.88	1899.93	39.45	32419.76	38.88	12625.17
RA	39.25	2046.23	39.95	38028.34	39.28	14476.10
Norm	38.94	1734.96	39.68	28780.25	38.98	11337.29

Day3-day7						
	Plasma		Heart		Lung	
	Time	Concentration	Time	Concentration	Time	Concentration
GRF	162.69	2445.39	163.53	42398.73	162.69	16409.35
GRFL	162.86	2498.87	163.63	45173.57	162.86	17255.99
MO	50.00	1046.85	50.53	17887.54	50.00	6950.55
NEC	162.39	2100.63	163.23	35628.83	162.39	13892.67
Obe	50.03	1277.70	50.64	21678.93	50.03	8450.27
Preg	49.96	1483.36	50.47	25359.27	49.96	9857.63
RA	162.66	1730.98	163.30	32362.16	162.69	12251.80
Norm	162.32	1351.45	162.99	22475.06	162.32	8819.68

GRF: renal impairment population, $30 \text{ mL/min} \leq \text{GRF} \leq 60 \text{ mL/min}$, GRFL: renal impairment population, $\text{GRF} \leq 30 \text{ mL/min}$, MO: morbidly obese population, NEC: geriatric Northern European Caucasians population, Obe: obese population, Preg: pregnant population, RA: rheumatoid arthritis population and Norm: healthy volunteers.

Table S7 The predicted maximum drug concentration and the corresponding time during two dosing periods of dosing regimen 12

Day1-day2						
	Plasma		Heart		Lung	
	Time	Concentration	Time	Concentration	Time	Concentration
GRF	39.41	2249.67	40.32	38773.87	39.45	15095.14
GRFL	39.58	2154.68	40.46	38786.24	39.62	14883.00
MO	40.39	1277.36	41.06	21781.90	40.39	8479.04
NEC	39.11	2208.87	40.12	37308.93	39.14	14619.62
Obe	39.65	1571.62	40.46	26590.57	39.68	10391.02
Preg	38.88	1899.93	39.45	32419.76	38.88	12625.17
RA	39.25	2046.23	39.95	38028.34	39.28	14476.10
Norm	38.94	1734.96	39.68	28780.25	38.98	11337.29

Day3-day7						
	Plasma		Heart		Lung	
	Time	Concentration	Time	Concentration	Time	Concentration
GRF	159.20	3011.65	160.10	52177.75	159.20	20208.71
GRFL	159.37	3053.59	160.21	55176.33	159.40	21087.04
MO	159.84	1248.37	160.54	21315.48	159.87	8285.17
NEC	158.86	2631.33	159.84	44609.61	158.89	17404.67
Obe	159.26	1616.70	160.04	27420.02	159.26	10689.13
Preg	158.66	1825.74	159.23	31201.37	158.69	12129.25
RA	159.06	2206.30	159.77	41202.94	159.10	15615.18
Norm	158.73	1751.89	159.47	29124.43	158.76	11435.58

GRF: renal impairment population, $30 \text{ mL/min} \leq \text{GRF} \leq 60 \text{ mL/min}$, GRFL: renal impairment population, $\text{GRF} \leq 30 \text{ mL/min}$, MO: morbidly obese population, NEC: geriatric Northern European Caucasians population, Obe: obese population, Preg: pregnant population, RA: rheumatoid arthritis population and Norm: healthy volunteers.

Table S8 The predicted maximum drug concentration and the corresponding time during three dosing periods of dosing regimen 15

Day1-day2						
	Plasma		Heart		Lung	
	Time	Concentration	Time	Concentration	Time	Concentration
GRF	39.41	2249.67	40.32	38773.87	39.45	15095.14
GRFL	39.58	2154.68	40.46	38786.24	39.62	14883.00
MO	40.49	1342.68	41.06	22990.67	40.52	8929.18
NEC	39.28	2106.65	40.02	35655.06	39.28	13925.49
Obe	39.78	1619.52	40.59	27463.21	39.82	10717.40
Preg	38.88	1899.93	39.45	32419.76	38.88	12625.17
RA	39.25	2046.23	39.95	38028.34	39.28	14476.10
Norm	38.94	1740.53	39.68	28886.88	38.94	11381.21
Day3						
	Plasma		Heart		Lung	
	Time	Concentration	Time	Concentration	Time	Concentration
GRF	63.17	2162.63	64.08	37414.48	63.20	14512.87
GRFL	63.34	2117.95	64.18	38235.69	63.37	14629.76
MO	51.34	1224.09	51.95	20976.04	51.37	8141.18
NEC	50.64	1948.63	51.37	33007.82	50.67	12881.62
Obe	50.90	1490.03	51.68	25285.41	50.90	9861.96
Preg	50.47	1690.49	51.01	28875.15	50.47	11233.77
RA	50.80	1836.95	51.48	34234.93	50.80	12996.79
Norm	50.50	1540.91	51.24	25618.57	50.54	10073.18
Day4-day7						
	Plasma		Heart		Lung	
	Time	Concentration	Time	Concentration	Time	Concentration
GRF	162.69	2513.02	163.50	43574.44	162.69	16863.18
GRFL	162.83	2569.98	163.63	46461.49	162.86	17747.04
MO	74.76	1062.97	75.37	18222.29	74.79	7069.30
NEC	162.42	1939.85	163.13	32906.24	162.42	12819.20
Obe	162.59	1372.82	163.33	23326.17	162.59	9083.97
Preg	74.26	1455.34	74.79	24887.82	74.26	9670.36
RA	162.66	1772.92	163.30	33149.20	162.66	12548.79
Norm	162.29	1403.57	162.99	23372.45	162.32	9168.29

GRF: renal impairment population, $30 \text{ mL/min} \leq \text{GRF} \leq 60 \text{ mL/min}$, GRFL: renal impairment population, $\text{GRF} \leq 30 \text{ mL/min}$, MO: morbidly obese population, NEC: geriatric Northern European Caucasians population, Obe: obese population, Preg: pregnant population, RA: rheumatoid arthritis population and Norm: healthy volunteers.

Table S9 The predicted maximum drug concentration and the corresponding time during three dosing periods of dosing regimen 16

Day1-day2						
	Plasma		Heart		Lung	
	Time	Concentration	Time	Concentration	Time	Concentration
GRF	39.35	2297.73	40.15	39719.37	39.38	15437.99
GRFL	39.58	2154.68	40.46	38786.24	39.62	14883.00
MO	40.49	1342.68	41.06	22990.67	40.52	8929.18
NEC	39.11	2208.87	40.12	37308.93	39.14	14619.62
Obe	39.65	1571.62	40.46	26590.57	39.68	10391.02
Preg	38.88	1899.93	39.45	32419.76	38.88	12625.17
RA	39.14	1986.77	39.78	36810.39	39.18	14009.43
Norm	38.94	1734.96	39.68	28780.25	38.98	11337.29
Day3-day4						
	Plasma		Heart		Lung	
	Time	Concentration	Time	Concentration	Time	Concentration
GRF	87.19	2395.72	87.96	41569.36	87.23	16096.81
GRFL	87.43	2355.83	88.27	42547.92	87.43	16271.27
MO	51.34	1224.09	51.95	20976.04	51.37	8141.18
NEC	86.92	2193.93	87.86	37180.00	86.92	14515.26
Obe	87.33	1459.59	88.10	24750.52	87.33	9651.30
Preg	86.69	1695.30	87.26	28972.93	86.69	11264.30
RA	87.02	1772.32	87.60	32919.68	87.02	12495.58
Norm	86.76	1579.95	87.50	26267.32	86.79	10316.93
Day5-day7						
	Plasma		Heart		Lung	
	Time	Concentration	Time	Concentration	Time	Concentration
GRF	162.69	2541.73	163.40	44169.19	162.69	17077.29
GRFL	162.83	2645.94	163.60	47837.34	162.86	18271.56
MO	98.78	1098.82	99.39	18836.60	98.78	7307.27
NEC	162.36	2216.24	163.23	37595.50	162.39	14657.09
Obe	98.52	1327.12	99.25	22523.18	98.55	8776.00
Preg	98.25	1509.21	98.78	25809.08	98.28	10027.64
RA	162.59	1629.86	163.16	30320.76	162.59	11492.42
Norm	162.29	1419.41	162.96	23607.98	162.32	9262.82

GRF: renal impairment population, $30 \text{ mL/min} \leq \text{GRF} \leq 60 \text{ mL/min}$, GRFL: renal impairment population, $\text{GRF} \leq 30 \text{ mL/min}$, MO: morbidly obese population, NEC: geriatric Northern European Caucasians population, Obe: obese population, Preg: pregnant population, RA: rheumatoid arthritis population and Norm: healthy volunteers.

Table S10 The predicted maximum drug concentration and the corresponding time during three dosing periods of adjusted dosing regimen for the two renal impairment population

GR1 (GRFL)						
	Plasma		Heart		Lung	
	Time	Concentration	Time	Concentration	Time	Concentration
Day1-Day2	39.51	1566.68	40.22	28073.30	39.51	10776.66
Day3	50.64	1381.43	51.31	24804.88	50.67	9502.08
Day4-Day7	75.23	1385.23	75.94	24893.62	75.26	9527.23
GR1 (GRF)						
	Plasma		Heart		Lung	
	Time	Concentration	Time	Concentration	Time	Concentration
Day1-Day2	39.35	1621.14	40.12	27781.00	39.35	10820.87
Day3	50.53	1407.72	51.21	24190.23	50.53	9395.78
Day4-Day7	75.06	1387.06	75.84	23859.07	75.10	9257.70
GR2 (GRFL)						
	Plasma		Heart		Lung	
	Time	Concentration	Time	Concentration	Time	Concentration
0-36h (1.5 d)	27.55	1748.91	28.26	31311.80	27.55	12030.55
36-72 h	38.44	1452.58	39.04	26079.72	38.44	9991.86
72-168 h	75.26	1446.13	75.94	25990.92	75.26	9946.02
GR2 (GRF)						
	Plasma		Heart		Lung	
	Time	Concentration	Time	Concentration	Time	Concentration
0-36h (1.5 d)	27.38	1822.69	28.16	31201.57	27.38	12166.46
36-72 h	38.30	1488.07	38.94	25569.37	38.30	9932.15
72-168 h	75.06	1443.20	75.84	24828.46	75.10	9632.38

GRF: renal impairment population, 30 mL/min≤GRF≤60 mL/min, GRFL: renal impairment population, GRF≤30 mL/min, MO: morbidly obese population, NEC: geriatric Northern European Caucasians population, Obe: obese population, Preg: pregnant population, RA: rheumatoid arthritis population and Norm: healthy volunteers.

Table S11 The predicted maximum drug concentration and the corresponding time during three dosing periods of adjusted dosing regimen for the elder population

NR1						
	Plasma		Heart		Lung	
	Time	Concentration	Time	Concentration	Time	Concentration
Day1-Day2	39.48	1651.75	40.32	27922.31	39.48	10933.66
Day3	63.00	1715.87	63.84	29043.59	63.00	11354.35
Day4-Day7	158.76	1610.98	159.60	27321.48	158.76	10654.24
NR2						
	Plasma		Heart		Lung	
	Time	Concentration	Time	Concentration	Time	Concentration
0-60 h (2.5 d)	51.24	1879.47	52.08	31776.97	51.24	12439.18
60-168 h	62.16	1630.82	63.00	27629.53	62.16	10790.07
NR3						
	Plasma		Heart		Lung	
	Time	Concentration	Time	Concentration	Time	Concentration
0-36h (1.5 d)	26.88	1875.80	28.56	31636.81	26.88	12413.85
36-168 h	158.76	1532.55	159.60	25986.39	158.76	10135.37

GRF: renal impairment population, $30 \text{ mL/min} \leq \text{GRF} \leq 60 \text{ mL/min}$, GRFL: renal impairment population, $\text{GRF} \leq 30 \text{ mL/min}$, MO: morbidly obese population, NEC: geriatric Northern European Caucasians population, Obe: obese population, Preg: pregnant population, RA: rheumatoid arthritis population and Norm: healthy volunteers.

Appendix A.2 Supplementary Figures

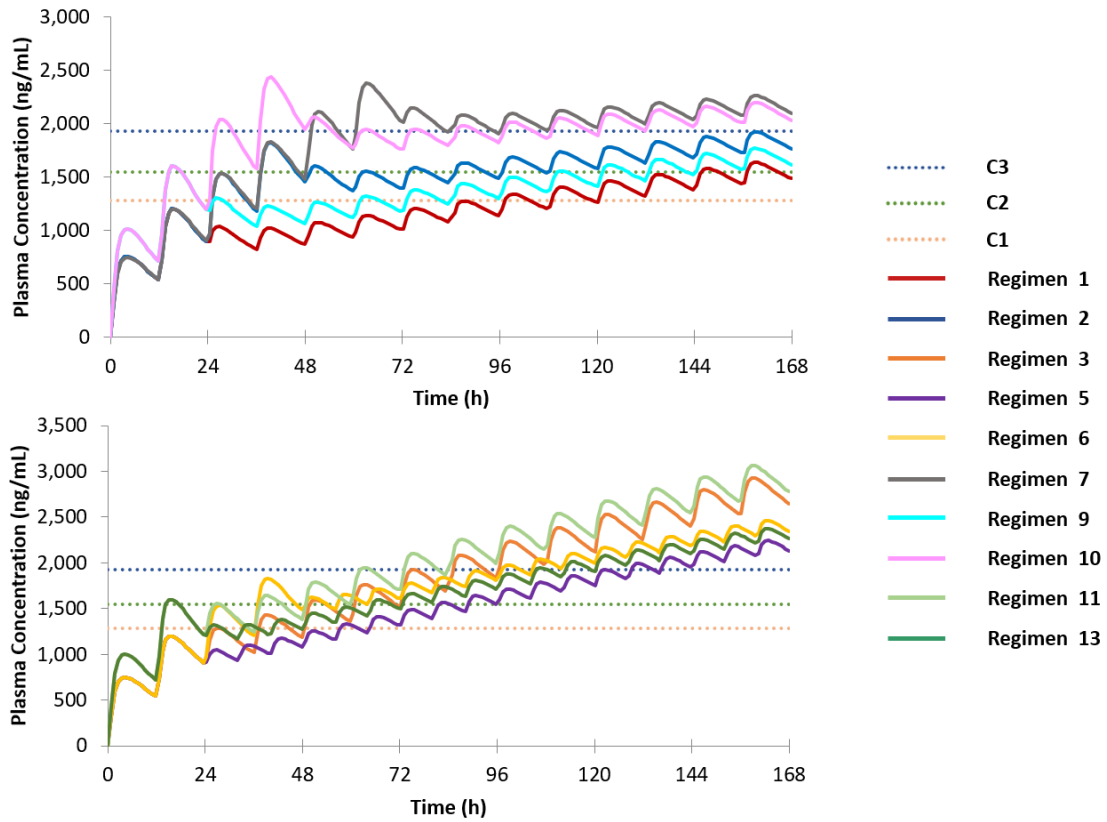


Figure S1 Predicted drug concentration profiles for the renal impairment population (GRF) in plasma under Regimens 1, 2, 3, 5, 6, 7, 9, 10, 11 and 13.

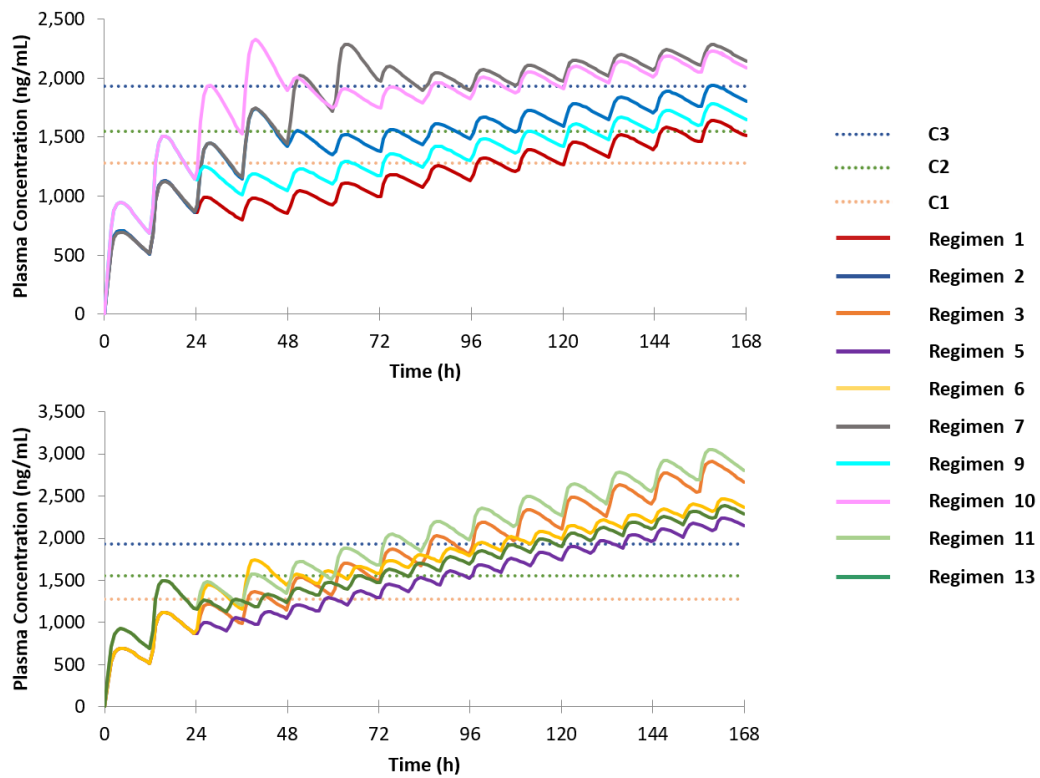


Figure S2 Predicted drug concentration profiles for the renal impairment population (GRFL) in plasma under Regimens 1, 2, 3, 5, 6, 7, 9, 10, 11 and 13.

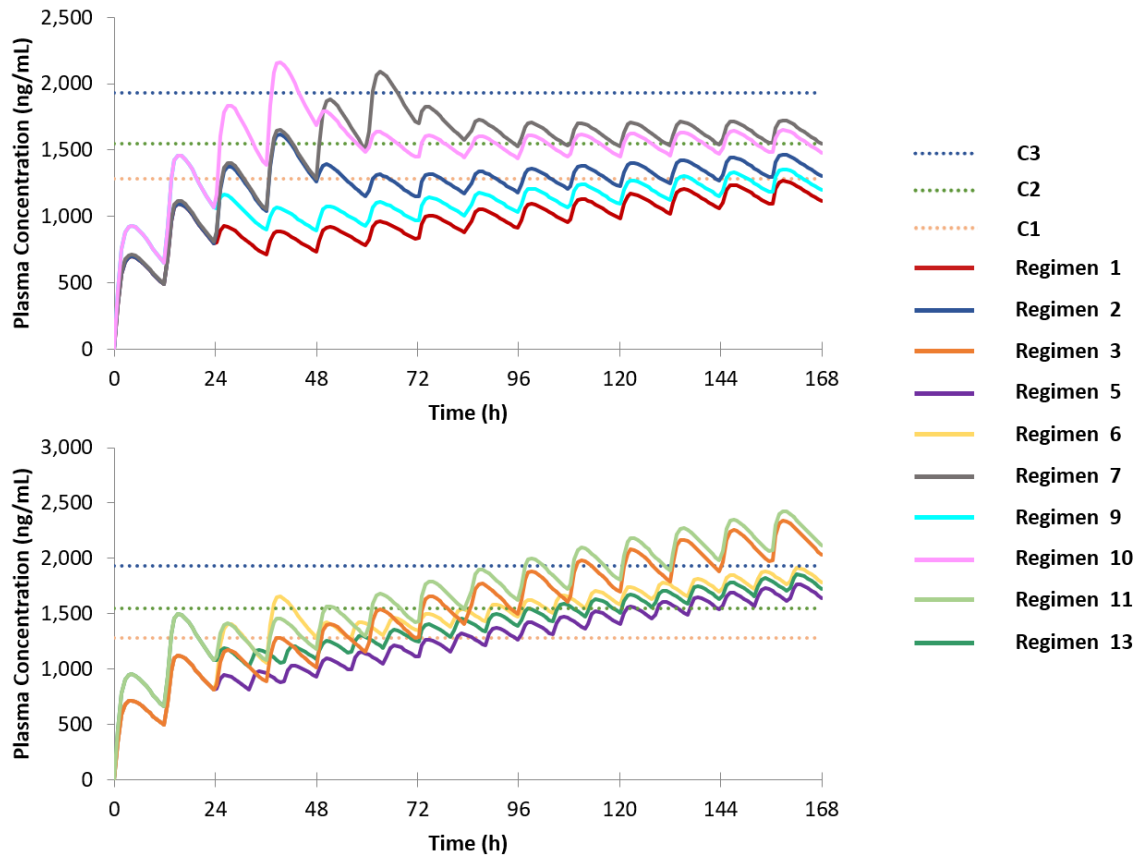


Figure S3 Predicted drug concentration profiles for the elder population (NEC) in plasma under Regimens 1, 2, 3, 5, 6, 7, 9, 10, 11 and 13.

Bibliography

- [1] K.J. Clerkin, J.A. Fried, J. Raikhelkar, G. Sayer, J.M. Griffin, A. Masoumi, S.S. Jain, D. Burkhoff, D. Kumaraiah, L. Rabbani, COVID-19 and cardiovascular disease, *Circulation* 141 (2020) 1648-1655.
- [2] Z.Y. Zu, M.D. Jiang, P.P. Xu, W. Chen, Q.Q. Ni, G.M. Lu, L.J. Zhang, Coronavirus Disease 2019 (COVID-19): A Perspective from China, *Radiology* 296 (2020) E15-E25. 10.1148/radiol.2020200490.
- [3] D. Plewczynski, M. Lazniewski, R. Augustyniak, K. Ginalski, Can We Trust Docking Results? Evaluation of Seven Commonly Used Programs on PDBbind Database, *J Comput Chem* 32 (2011) 742-755. 10.1002/jcc.21643.
- [4] L. Fang, G. Karakiulakis, M. Roth, Are patients with hypertension and diabetes mellitus at increased risk for COVID-19 infection?, *The Lancet. Respiratory Medicine* 8 (2020) e21.
- [5] W.-j. Guan, Z.-y. Ni, Y. Hu, W.-h. Liang, C.-q. Ou, J.-x. He, L. Liu, H. Shan, C.-l. Lei, D.S. Hui, Clinical characteristics of coronavirus disease 2019 in China, *New England journal of medicine* 382 (2020) 1708-1720.
- [6] W. Guo, M. Li, Y. Dong, H. Zhou, Z. Zhang, C. Tian, R. Qin, H. Wang, Y. Shen, K. Du, Diabetes is a risk factor for the progression and prognosis of COVID-19, *Diabetes/metabolism research and reviews* (2020) e3319.
- [7] L.G. Ferreira, R.N. dos Santos, G. Oliva, A.D. Andricopulo, Molecular Docking and Structure-Based Drug Design Strategies, *Molecules* 20 (2015) 13384-13421. 10.3390/molecules200713384.
- [8] C.D. Spinner, R.L. Gottlieb, G.J. Criner, J.R.A. López, A.M. Cattelan, A.S. Viladomiu, O. Ogbuagu, P. Malhotra, K.M. Mullane, A. Castagna, Effect of remdesivir vs standard care on clinical status at 11 days in patients with moderate COVID-19: a randomized clinical trial, *Jama* 324 (2020) 1048-1057.
- [9] J.D. Goldman, D.C. Lye, D.S. Hui, K.M. Marks, R. Bruno, R. Montejano, C.D. Spinner, M. Galli, M.-Y. Ahn, R.G. Nahass, Remdesivir for 5 or 10 days in patients with severe Covid-19, *New England Journal of Medicine* (2020).
- [10] J.M. Sanders, M.L. Monogue, T.Z. Jodlowski, J.B. Cutrell, Pharmacologic Treatments for Coronavirus Disease 2019 (COVID-19): A Review, *JAMA* 323 (2020) 1824-1836. 10.1001/jama.2020.6019.
- [11] R.E. Ferner, J.K. Aronson, Chloroquine and hydroxychloroquine in covid-19, *British Medical Journal Publishing Group*, 2020.
- [12] L. Dong, S. Hu, J. Gao, Discovering drugs to treat coronavirus disease 2019 (COVID-19), *Drug discoveries & therapeutics* 14 (2020) 58-60.
- [13] R.S. Cvetkovic, K.L. Goa, Lopinavir/ritonavir, *Drugs* 63 (2003) 769-802.
- [14] S.G.V. Rosa, W.C. Santos, Clinical trials on drug repositioning for COVID-19 treatment, *Revista Panamericana de Salud Pública* 44 (2020) e40.
- [15] P.J. Eddershaw, A.P. Beresford, M.K. Bayliss, ADME/PK as part of a rational approach to drug discovery, *Drug Discovery Today* 5 (2000) 409-414. [https://doi.org/10.1016/S1359-6446\(00\)01540-3](https://doi.org/10.1016/S1359-6446(00)01540-3).
- [16] J. Lu, M.-R. Goldsmith, C.M. Grulke, D.T. Chang, R.D. Brooks, J.A. Leonard, M.B. Phillips, E.D. Hypes, M.J. Fair, R. Tornero-Velez, Developing a physiologically-based pharmacokinetic

model knowledgebase in support of provisional model construction, PLoS computational biology 12 (2016).

[17] X. Zhuang, C. Lu, PBPK modeling and simulation in drug research and development, *Acta Pharmaceutica Sinica B* 6 (2016) 430-440.

[18] L. Lin, H. Wong, Predicting oral drug absorption: mini review on physiologically-based pharmacokinetic models, *Pharmaceutics* 9 (2017) 41.

[19] M. Jamei, S. Marciniak, K. Feng, A. Barnett, G. Tucker, A. Rostami-Hodjegan, The Simcyp® Population-based ADME Simulator, *Expert Opinion on Drug Metabolism & Toxicology* 5 (2009) 211-223. 10.1517/17425250802691074.

[20] S.F. Hassan, U. Rashid, F.L. Ansari, Z. Ul-Haq, Bioisosteric approach in designing new monastrol derivatives: an investigation on their ADMET prediction using in silico derived parameters, *Journal of Molecular Graphics and Modelling* 45 (2013) 202-210.

[21] D. Hecht, G.B. Fogel, Computational intelligence methods for ADMET prediction, *Front Drug Des Discov* 4 (2009) 351-377.

[22] Z. Sahraei, M. Shabani, S. Shokouhi, A. Saffaei, Aminoquinolines against coronavirus disease 2019 (COVID-19): chloroquine or hydroxychloroquine, *Int J Antimicrob Agents* 105945 (2020).

[23] G. Klinger, Y. Morad, C.A. Westall, C. Laskin, K.A. Spitzer, G. Koren, S. Ito, R.J. Buncic, Ocular toxicity and antenatal exposure to chloroquine or hydroxychloroquine for rheumatic diseases, *The lancet* 358 (2001) 813-814.

[24] M. Motta, A. Tincani, D. Faden, E. Zinzini, A. Lojacono, A. Marchesi, M. Frassi, C. Biasini, S. Zatti, G. Chirico, Follow-up of infants exposed to hydroxychloroquine given to mothers during pregnancy and lactation, *Journal of perinatology* 25 (2005) 86-89.

[25] I. Ben-Zvi, S. Kivity, P. Langevitz, Y. Shoenfeld, Hydroxychloroquine: from malaria to autoimmunity, *Clinical reviews in allergy & immunology* 42 (2012) 145-153.

[26] D.E. Furst, Pharmacokinetics of hydroxychloroquine and chloroquine during treatment of rheumatic diseases, *Lupus* 5 (1996) 11-15.

[27] P. Colson, J.-M. Rolain, J.-C. Lagier, P. Brouqui, D. Raoult, Chloroquine and hydroxychloroquine as available weapons to fight COVID-19, *Int J Antimicrob Agents* 105932 (2020).

[28] Food, D. Administration, *Plaquenil® Hydroxychloroquine Sulfate Tablets, USP*, 2018.

[29] M. Guastalegname, A. Vallone, Could chloroquine/hydroxychloroquine be harmful in coronavirus disease 2019 (COVID-19) treatment?, *Clinical Infectious Diseases* (2020).

[30] J. Yazdany, A.H. Kim, Use of hydroxychloroquine and chloroquine during the COVID-19 pandemic: what every clinician should know, *American College of Physicians*, 2020.

[31] M. Garcia-Cremades, B.P. Solans, E. Hughes, J.P. Ernest, E. Wallender, F. Aweeka, A.F. Luetkemeyer, R.M. Savic, Optimizing hydroxychloroquine dosing for patients with COVID-19: An integrative modeling approach for effective drug repurposing, *Clinical Pharmacology & Therapeutics* (2020).

[32] P. Gautret, J.-C. Lagier, P. Parola, L. Meddeb, M. Mailhe, B. Doudier, J. Courjon, V. Giordanengo, V.E. Vieira, H.T. Dupont, Hydroxychloroquine and azithromycin as a treatment of COVID-19: results of an open-label non-randomized clinical trial, *International journal of antimicrobial agents* (2020) 105949.

[33] P. Gautret, J.-C. Lagier, P. Parola, L. Meddeb, J. Sevestre, M. Mailhe, B. Doudier, C. Aubry, S. Amrane, P. Seng, Clinical and microbiological effect of a combination of hydroxychloroquine and azithromycin in 80 COVID-19 patients with at least a six-day follow up: A pilot observational study, *Travel medicine and infectious disease* (2020) 101663.

- [34] J.-C. Lagier, F. Fenollar, H. Lepidi, R. Giorgi, M. Million, D. Raoult, Treatment of classic Whipple's disease: from in vitro results to clinical outcome, *Journal of Antimicrobial Chemotherapy* 69 (2014) 219-227.
- [35] D. Zhou, S.-M. Dai, Q. Tong, COVID-19: a recommendation to examine the effect of hydroxychloroquine in preventing infection and progression, *Journal of Antimicrobial Chemotherapy* (2020).
- [36] K.P. Collins, K.M. Jackson, D.L. Gustafson, Hydroxychloroquine: A Physiologically-Based Pharmacokinetic Model in the Context of Cancer-Related Autophagy Modulation, *Journal of Pharmacology and Experimental Therapeutics* 365 (2018) 447. 10.1124/jpet.117.245639.
- [37] M. Zhang, X. Yao, Z. Hou, X. Guo, S. Tu, Z. Lei, Z. Yu, X. Liu, C. Cui, X. Chen, N. Shen, C. Song, J. Qiao, X. Xiang, H. Li, D. Liu, Development of a Physiologically Based Pharmacokinetic Model for Hydroxychloroquine and Its Application in Dose Optimization in Specific COVID-19 Patients, *Front Pharmacol* 11 (2020) 585021. 10.3389/fphar.2020.585021.
- [38] A.A. Toropov, A.P. Toropova, D.V. Mukhamedzhanova, I. Gutman, Simplified molecular input line entry system (SMILES) as an alternative for constructing quantitative structure-property relationships (QSPR), (2005).
- [39] D. Bajusz, A. Rácz, K. Héberger, Why is Tanimoto index an appropriate choice for fingerprint-based similarity calculations?, *Journal of cheminformatics* 7 (2015) 20.
- [40] A. Sharma, S.P. Lal, Tanimoto based similarity measure for intrusion detection system, *Journal of Information Security* 2 (2011) 195.
- [41] B. Agoram, W.S. Woltosz, M.B. Bolger, Predicting the impact of physiological and biochemical processes on oral drug bioavailability, *Advanced drug delivery reviews* 50 (2001) S41-S67.
- [42] L. Franceschi, A. Faggiani, M. Furlanut, A simple method to monitor serum concentrations of fluoxetine and its major metabolite for pharmacokinetic studies, *Journal of pharmaceutical and biomedical analysis* 49 (2009) 554-557.
- [43] D.L. D'Souza, D.C. Dimmitt, D.K. Robbins, J. Nezamis, L. Simms, K.M. Koch, Effect of alosetron on the pharmacokinetics of fluoxetine, *The Journal of Clinical Pharmacology* 41 (2001) 455-458.
- [44] A. Tropsha, P. Gramatica, V.K. Gombar, The importance of being earnest: validation is the absolute essential for successful application and interpretation of QSPR models, *QSAR & Combinatorial Science* 22 (2003) 69-77.
- [45] T. Chai, R.R. Draxler, Root mean square error (RMSE) or mean absolute error (MAE)?, *GMDD* 7 (2014) 1525-1534.
- [46] N. Gobeau, R. Stringer, S. De Buck, T. Tuntland, B. Faller, Evaluation of the GastroPlus™ advanced compartmental and transit (acat) model in early discovery, *Pharmaceutical research* 33 (2016) 2126-2139.
- [47] H. Carlsson, K. Hjorton, S. Abujrais, L. Rönnblom, T. Åkerfeldt, K. Kultima, Measurement of hydroxychloroquine in blood from SLE patients using LC-HRMS—evaluation of whole blood, plasma, and serum as sample matrices, *Arthritis Research & Therapy* 22 (2020) 125. 10.1186/s13075-020-02211-1.
- [48] S. Tett, D. Cutler, R. Day, K. Brown, Bioavailability of hydroxychloroquine tablets in healthy volunteers, *British journal of clinical pharmacology* 27 (1989) 771-779.
- [49] S. Tett, D. Cutler, R. Day, K. Brown, A dose-ranging study of the pharmacokinetics of hydroxy-chloroquine following intravenous administration to healthy volunteers, *British journal of clinical pharmacology* 26 (1988) 303-313.

- [50] J.Y. Lee, N. Vinayagamoorthy, K. Han, S.K. Kwok, J.H. Ju, K.S. Park, S.H. Jung, S.W. Park, Y.J. Chung, S.H. Park, Association of polymorphisms of cytochrome P450 2D6 with blood hydroxychloroquine levels in patients with systemic lupus erythematosus, *Arthritis & Rheumatology* 68 (2016) 184-190.
- [51] S. Quraishi, B.T. Reed, R.M. Duvoisin, W.R. Taylor, Selective activation of mGluR8 receptors modulates retinal ganglion cell light responses, *Neuroscience* 166 (2010) 935-941. 10.1016/j.neuroscience.2010.01.027.
- [52] A. Crowe, K.F. Ilett, H.A. Karunajeewa, K.T. Batty, T.M.E. Davis, Role of P Glycoprotein in Absorption of Novel Antimalarial Drugs, *Antimicrobial Agents and Chemotherapy* 50 (2006) 3504. 10.1128/AAC.00708-06.
- [53] C. Xu, L. Zhu, T. Chan, X. Lu, W. Shen, M.C. Madigan, M.C. Gillies, F. Zhou, Chloroquine and Hydroxychloroquine Are Novel Inhibitors of Human Organic Anion Transporting Polypeptide 1A2, *J Pharm Sci* 105 (2016) 884-890. 10.1002/jps.24663.
- [54] A. Crowe, K.F. Ilett, H.A. Karunajeewa, K.T. Batty, T.M. Davis, Role of P glycoprotein in absorption of novel antimalarial drugs, *Antimicrobial agents and chemotherapy* 50 (2006) 3504-3506.
- [55] K.P. Collins, K.M. Jackson, D.L. Gustafson, Hydroxychloroquine: a physiologically-based pharmacokinetic model in the context of cancer-related autophagy modulation, *Journal of Pharmacology and Experimental Therapeutics* 365 (2018) 447-459.
- [56] M.M. Abraham, Hydroxychloroquine dimers as inhibitors of Plasmodium falciparum chloroquine resistant transporter and P-glycoprotein, (2015).
- [57] D. Van Der Heijde, P. Van Riel, F. Gribnau, I. Nuver-Zwart, L. Van De Putte, Effects of hydroxychloroquine and sulphasalazine on progression of joint damage in rheumatoid arthritis, *The Lancet* 333 (1989) 1036-1038.
- [58] S.C. Laizure, B. Meibohm, K. Nelson, F. Chen, Z.Y. Hu, R.B. Parker, Comparison of caffeine disposition following administration by oral solution (energy drink) and inspired powder (AeroShot) in human subjects, *British journal of clinical pharmacology* 83 (2017) 2687-2694.
- [59] F. Qiu, G. Wang, Y. Zhao, H. Sun, G. Mao, J. Sun, Effect of danshen extract on pharmacokinetics of theophylline in healthy volunteers, *British journal of clinical pharmacology* 65 (2008) 270-274.
- [60] K.i. Sugimoto, M. Ohmori, S. Tsuruoka, K. Nishiki, A. Kawaguchi, K.i. Harada, M. Arakawa, K.i. Sakamoto, M. Masada, I. Miyamori, Different effects of St John's wort on the pharmacokinetics of simvastatin and pravastatin, *Clinical Pharmacology & Therapeutics* 70 (2001) 518-524.
- [61] S.A. Chalon, J.P. Desager, K.A. DeSante, R.F. Frye, J. Witcher, A.J. Long, J.M. Sauer, J.L. Golnez, B.P. Smith, H.R. Thomasson, Effect of hepatic impairment on the pharmacokinetics of atomoxetine and its metabolites, *Clinical Pharmacology & Therapeutics* 73 (2003) 178-191.
- [62] E. NELSON, J.R. POWELL, K. CONRAD, K. LIKES, J. BYERS, S. BAKER, D. PERRIER, Phenobarbital pharmacokinetics and bioavailability in adults, *The Journal of Clinical Pharmacology* 22 (1982) 141-148.
- [63] P. Wedlund, W. Aslanian, E. Jacqz, C. McAllister, R. Branch, G. Wilkinson, Phenotypic differences in mephenytoin pharmacokinetics in normal subjects, *Journal of Pharmacology and Experimental Therapeutics* 234 (1985) 662-669.
- [64] D.J. Greenblatt, J.S. Harmatz, L.L. von Moltke, C.E. Wright, A.L.B. Durol, L.M. Harrel-Joseph, R.I. Shader, Comparative kinetics and response to the benzodiazepine agonists triazolam

and zolpidem: evaluation of sex-dependent differences, *Journal of Pharmacology and Experimental Therapeutics* 293 (2000) 435-443.

[65] K. Otani, N. Yasui, H. Furukori, S. Kaneko, H. Tasaki, T. Ohkubo, T. Nagasaki, K. Sugawara, K. Hayashi, Relationship between single oral dose pharmacokinetics of alprazolam and triazolam, *International clinical psychopharmacology* 12 (1997) 153-157.

[66] B. Link, M. Haschke, N. Grignaschi, M. Bodmer, Y.Z. Aschmann, M. Wenk, S. Krähenbühl, Pharmacokinetics of intravenous and oral midazolam in plasma and saliva in humans: usefulness of saliva as matrix for CYP3A phenotyping, *British journal of clinical pharmacology* 66 (2008) 473-484.

[67] X. Chen, G. Jacobs, M. de Kam, J. Jaeger, J. Lappalainen, P. Maruff, M.A. Smith, A.J. Cross, A. Cohen, J. Van Gerven, The central nervous system effects of the partial GABA-A α_2 , 3-selective receptor modulator AZD7325 in comparison with lorazepam in healthy males, *British journal of clinical pharmacology* 78 (2014) 1298-1314.

[68] T. East, D. Dye, Determination of dextromethorphan and metabolites in human plasma and urine by high-performance liquid chromatography with fluorescence detection, *Journal of Chromatography B: Biomedical Sciences and Applications* 338 (1985) 99-112.

[69] J.N. Connarn, S. Flowers, M. Kelly, R. Luo, K.M. Ward, G. Harrington, I. Moncion, M. Kamali, M. McInnis, M.R. Feng, Pharmacokinetics and pharmacogenomics of bupropion in three different formulations with different release kinetics in healthy human volunteers, *The AAPS journal* 19 (2017) 1513-1522.

[70] T. Pringle, R. Francis, P. East, R. Shanks, Pharmacodynamic and pharmacokinetic studies on bufuralol in man, *British journal of clinical pharmacology* 22 (1986) 527-534.

[71] K.W. Kolb, W.R. Garnett, R.E. Small, G.W. Vetovec, B.J. Kline, T. Fox, Effect of cimetidine on quinidine clearance, *Therapeutic drug monitoring* 6 (1984) 306-312.

[72] D.A. Ciraulo, J.G. Barnhill, J.H. Jaffe, Clinical pharmacokinetics of imipramine and desipramine in alcoholics and normal volunteers, *Clinical Pharmacology & Therapeutics* 43 (1988) 509-518.

[73] S. Madani, D. Barilla, J. Cramer, Y. Wang, C. Paul, Effect of terbinafine on the pharmacokinetics and pharmacodynamics of desipramine in healthy volunteers identified as cytochrome P450 2D6 (CYP2D6) extensive metabolizers, *The Journal of Clinical Pharmacology* 42 (2002) 1211-1218.

[74] H.-S. Lim, J.-S. Im, J.-Y. Cho, K.-S. Bae, T.A. Klein, J.-S. Yeom, T.-S. Kim, J.-S. Choi, I.-J. Jang, J.-W. Park, Pharmacokinetics of hydroxychloroquine and its clinical implications in chemoprophylaxis against malaria caused by *Plasmodium vivax*, *Antimicrobial Agents and Chemotherapy* 53 (2009) 1468-1475.

[75] J.M. Molina, C. Delaugerre, J. Le Goff, B. Mela-Lima, D. Ponscarne, L. Goldwirt, N. de Castro, No evidence of rapid antiviral clearance or clinical benefit with the combination of hydroxychloroquine and azithromycin in patients with severe COVID-19 infection, *Med Mal Infect* 50 (2020) 30085-30088.

[76] J. Chen, D. LIU, L. LIU, P. LIU, Q. XU, L. XIA, Y. LING, D. HUANG, S. SONG, D. ZHANG, A pilot study of hydroxychloroquine in treatment of patients with common coronavirus disease-19 (COVID-19), *Journal of Zhejiang University (Medical Science)* 49 (2020) 0-0.

[77] K. Gbinigie, K. Frie, Should chloroquine and hydroxychloroquine be used to treat COVID-19? A rapid review, *BJGP open* (2020).

- [78] W. Tang, Z. Cao, M. Han, Z. Wang, J. Chen, W. Sun, Y. Wu, W. Xiao, S. Liu, E. Chen, Hydroxychloroquine in patients with COVID-19: an open-label, randomized, controlled trial, *MedRxiv* (2020).
- [79] S.A. Bero, A.K. Muda, Y.-H. Choo, N.A. Muda, S.F. Pratama, Weighted Tanimoto Coefficient for 3D Molecule Structure Similarity Measurement, *arXiv preprint arXiv:1806.05237* (2018).
- [80] U. Food, D. Administration, Fact sheet for health care providers: emergency use authorization (EUA) of hydroxychloroquine sulfate supplied from the strategic national stockpile for treatment of COVID-19 in certain hospitalized patients, 2020.
- [81] S. Tsujimura, K. Saito, M. Nawata, S. Nakayamada, Y. Tanaka, Overcoming drug resistance induced by P-glycoprotein on lymphocytes in patients with refractory rheumatoid arthritis, *Annals of the rheumatic diseases* 67 (2008) 380-388.
- [82] Z. Tylutki, S. Polak, Plasma vs heart tissue concentration in humans—literature data analysis of drugs distribution, *Biopharm. Drug Disposition* 36 (2015) 337-351.
- [83] B. Owens, Excitement around hydroxychloroquine for treating COVID-19 causes challenges for rheumatology, *The Lancet Rheumatology* 2 (2020) e257.